CAL LAB

THE INTERNATIONAL JOURNAL OF METROLOGY

Tolerances for Non-Linear Analog Resistance Scales

Progress in the Theory of the Laminar Tube Thermal Flow Sensor

Leveraging LEAN in the Laboratory

2014
JANUARY
FEBRUARY
MARCH

CAL LAB
THE INTERNATIONAL JOURNAL OF METROLOGY

Volume 21, Number 1

www.callabmag.com

FEATURES

DEPARTMENTS

ON THE COVER: A Technician adjusts the steps of the JJ- Josephson Junction Array Primary Voltage Standard at the Agilent Technologies Primary Standards Lab in Loveland, Colorado.

CALENDAR

CONFERENCES & MEETINGS 2014

Mar 3-5 South East Asia Flow Measurement Conference. Kuala Lumpur, Malaysia. www.tuvnel.com.

Mar 11-13 International Conference on Surface Metrology (ICSM). Hamburg, Germany. http://www.biologie.uni-hamburg.de/zim/icsm2014/.

Mar 12-14 Measurement Science Conference (MSC). Long Beach, CA. Global Economic Challenges Drive Operational Change In Metrology. www.msc-conf.com.

Mar 24-26 Mathematics and Statistics for Metrology 2014. Berlin, Germany. http://www.ptb.de/cms/fachabteilungen/abt8/fb-84/mathmet-2014.html

Mar 27-28 Metromeet 2014. Bilbao, Spain. The 10th International Conference on Industrial Dimensional Metrology. http://www.metromeet.org/en/index.php

Mar 31-Apr 2 FORUMESURE. Pretoria, South Africa. FORUMESURE will takes place at the same time and same location as the conference CAFMET 2014. http://www.forumesure.com/.

Mar 31-Apr 3 CAFMET 2014. Pretoria, South Africa. The 5th International Metrology Conference. http://www.cafmet2014.com/.

May 12-15 IEEE I&M International Instrumentation and Measurement Technology Conference (I2MTC 2014). Montevideo, Uruguay. http://imtc.ieee-ims.org/

May 13-16 ESTECH 2014. San Antonio, TX. "Launching Into the Future." http://www.iest.org.

May 29-30 IEEE Workshop on Metrology for Aerospace (MetroAeroSpace). Benevento, Italy. http://www.metroaerospace.org.

Jun 26-27 ASPE/ASPEN Summer Topical Meeting. Kohala Coast, HI. Manufacture and Metrology of Freeform and Off-Axis Axisymmetric Surfaces. http://aspe.net.

Jul 15-17 North American Custody Transfer Measurement Conference. Denver, CO. Colorado Engineering Experiment Station, Inc. (CEESI). http://www.ceesi.com/Training/CustodyTransferMeasurementConference.aspx.

Jul 28-31 NCSL International Workshop & Symposium. Orlando, FL. Measurement Science and the Environment. www.ncsli.org.

CAL LAB
THE INTERNATIONAL JOURNAL OF METROLOGY

PUBLISHER
MICHAEL L. SCHWARTZ

EDITOR
SITA P. SCHWARTZ

CAL LAB
PO Box 111113
Aurora, CO 80042
TEL 303-317-6670 • FAX 303-317-5295
office@callabmag.com
www.callabmag.com

Subscription fees for 1 year (4 issues)
$50 for USA, $55 Mexico/Canada,
$65 all other countries.
Visit **www.callabmag.com**
to subscribe.

Printed in the USA.

ISSN No. 1095-4791

EDITOR'S DESK

We Are Changed

2014 marks the 100th anniversary of the beginning WWI. This fact just occurred to me one night after a strong glass of whiskey and soda and so the meaningfulness was amplified. The human race was forever changed by the Great War, yet it seems forgotten. WWII is still part of our living memory and still the backdrop of current movies, books, etc. But aside from PBS Sunday night airings of "Downton Abbey," the subject of WWI never comes up. My first field trip in the 7th grade was to the Stanford University Library to view recently restored footage of trench warfare from WWI. I had to look away at one point, unable to process what my eyes were seeing. In the 8th grade, our English teacher moved quickly and in depth to WWII, sparking a series of really bad dreams. What I got out of the lessons was that there is no such thing as black and white, good or evil—just human beings living with the consequences of daily events. Let us not forget the millions who lost their families, land, and lives to violence, disease, and famine. The Great War marked the end of those living in isolation away from everyone else's problems. Now, no one is immune and everyone is engaged.

Though not nearly dramatic, 2014 actually marks another anniversary… Cal Lab Magazine is 20 years old! If Cal Lab Magazine was a human baby, it would be driving its own car and dusting off a yellowed copy of "Old Mr. Boston" in anticipation of turning 21. I've been working on a complete index of Cal Lab Magazine published articles, including abstracts. Through all the cutting and pasting, the topics are similar throughout the past 20 years. The measurement science industry has seen some earth-shaking events these past 20 years, such as the kilogram standard change and that NCLSI conference in 2011, while the same issues, such as accreditation, the effect of government cut-backs, and lack of qualified technicians still exist today.

Most changes are those that seem to press into the measurement world from the outside, such as the evolution of computers (particularly communications equipment) and increase of software—drivers, firmware, and automation. But the *biggest* difference between then and now is how we use the INTERNET. No longer are we bound to uploading changes from our laptop when we get back to the lab or office. Quickly, we've gone from our company's "intranet" to the "cloud." And no more wires and cables hiding under carpets and rubber strips between offices… everything is wireless. In another 20 years, I suspect we will not recognize ourselves.

Some things don't change though. For that reason, Tom Morgan has hooked us up with this issue's Metrology 101 article on calculating the resistance tolerances for non-linear, analog resistance scales. Thomas Maginnis kindly shared his article on laminar thermal flow sensor technology, "Progress in the Theory of the Laminar Tube Thermal Flow Sensor." And, while we've let lapse inclusion of procedural or lab management articles, this issue picks up with Dean Williams' article "Leveraging LEAN in the Laboratory."

In whatever form Cal Lab Magazine takes in another 20 years, we hope you will keep reading!

Cheers,

Sita P. Schwartz
Editor

SEMINARS: Online & Independent Study

ASQ CCT (Certified Calibration Technician) Exam Preparation Program. Learning Measure. http://www.learningmeasure.com/.

AC-DC Metrology– Self-Paced Online Training. Fluke Training. http://us.flukecal.com/training/courses.

Basic Measurement Concepts Program. Learning Measure. http://www.learningmeasure.com/.

Basic Measuring Tools – Self Directed Learning. The QC Group, http://www.qcgroup.com/sdl/.

Basic RF and Microwave Program. Learning Measure. http://www.learningmeasure.com/.

Certified Calibration Technician – Self-study Course. J&G Technology. http://www.jg-technology.com/selfstudy.html.

Introduction to Measurement and Calibration – Online Training. The QC Group, http://www.qcgroup.com/online/.

Intro to Measurement and Calibration – Self-Paced Online Training. Fluke Training. http://us.flukecal.com/training/courses.

ISO/IEC 17025 Accreditation Courses. WorkPlace Training, tel (612) 308-2202, info@wptraining.com, http://www.wptraining.com/.

Measurement Uncertainty – Self-Paced Online Training. Fluke Training. http://us.flukecal.com/training/courses.

Measurement Uncertainty Analysis – Online Training. The QC Group, http://www.qcgroup.com/online/.

Metrology for Cal Lab Personnel– Self-Paced Online Training. Fluke Training. http://us.flukecal.com/training/courses.

Metrology Concepts. QUAMETEC Institute of Measurement Technology. http://www.QIMTonline.com.

Precision Dimensional Measurement – Online Training. The QC Group, http://www.qcgroup.com/online/.

Precision Measurement Series Level 1 & 2. WorkPlace Training, http://www.wptraining.com/.

Precision Electrical Measurement – Self-Paced Online Training. Fluke Training. http://us.flukecal.com/training/courses.

Vibration and Shock Testing. Equipment Reliability Institute, http://www.equipment-reliability.com/distance_learning.html.

Magnetic Field Measurement

Fluxgate Transducers

High Sensitivity for Low Fields

Mag648/649

Mag690

Mag-03MS

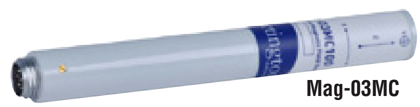

Mag-03MC

One and Three-axis Transducers with ±10V (±3V Mag640) analog outputs for each axis. For environmental field monitoring, mapping and active cancellation. Cryogenic sensors available.

Field Ranges	70, 100, 250, 500, 1000µT
Frequency Response	dc to 3kHz (-3dB) (Mag03), dc to >1kHz (Mag690, Mag649)
Noise Level	< 20pTrms/√Hz at 1Hz (Mag690), < 10pTrms/√Hz at 1Hz (Mag649), < 12pTrms/√Hz at 1Hz (Mag03 standard), < 6pTrms/√Hz at 1Hz (Mag03 low noise),

Hall Analog Transducers

Analog Output for Mapping or Control

One-, Two- and Three-axis Transducers with ±10V analog outputs for each axis.

Field Ranges	20mT, 200mT, 2T, 5T, 10T, 20T
Accuracy	±1% or ±0.1%
Frequency Response	dc to 2.5kHz (-3dB); Special to 25kHz
White Noise at >10Hz	0.12µT/√Hz for 2T range (Y-axis), 2µT/√Hz for 2T range (3-axis)

Hall Transducer Probe Packages

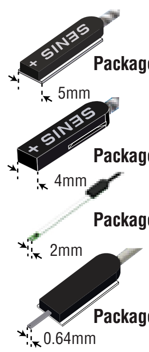

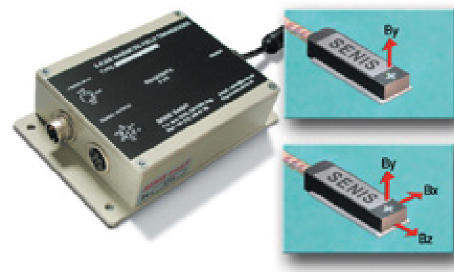

SENIS magnetic & current measurement

Field Probes with USB Interface

USB Connector, 3-Axis. Handheld PDA Option

For: Accurate mapping of magnetic fields. Pre-installation site surveys for magnetically sensitive equipment. Post-installation surveys of the dc and ac fringe fields of large magnets and magnetic assemblies. Field harmonic measurements over time for non-invasive load and condition monitoring of ac power assemblies like tranformers and motors. Complete with software for LabVIEW.

Fluxgate Probe	**TFM1186**
Field Range	±100µT
Noise	5nT p-p, 8 nT RMS (2kSPS, no averaging); 4nT p-p (100x averaging)

Hall Probe	**THM1176-LF**	**THM1176-MF**	**THM1176-HF**
Field Ranges	±8mT	±0.1T, 0.3T, 1T, 3T	±0.1T, 0.5T, 3T, 20T
Resolution	2µT	0.1mT	0.3mT on 3T range

METROLAB

TFM1186 Fluxgate Probe

THM1176 Hall Probe

NMR Teslameter

Mapping and Calibration Standard

For field calibration, mapping and control with high resolution, very high stability and absolute accuracy.

Field Ranges	from 0.04T to 13.7T
Resolution	±0.1µT or 1Hz (proton sample)
Absolute Accuracy	±5ppm

RS-232C and IEEE-488 Interfaces

Multiprobe NMR arrays for precision mapping of large magnets

PT2025

METROLAB

CALENDAR

SEMINARS: Dimensional

Mar 3-4, 2014 Hands-On Gage Calibration and Repair Workshop. Anaheim, CA. IICT Enterprises LLC. http://www.iictenterprisesllc.com/.

Mar 4, 2014 Dimensional Metrology: Applications and Techniques. Westford, MA. Mitutoyo Institute of Metrology. http://www.mitutoyo.com/support/mitutoyo-institute-of-metrology/.

Mar 6, 2014 Gage Calibration Systems and Methods. Westford, MA. Mitutoyo Institute of Metrology. http://www.mitutoyo.com/support/mitutoyo-institute-of-metrology/.

Mar 6-7, 2014 Hands-On Gage Calibration and Repair Workshop. San Jose, CA. IICT Enterprises LLC. http://www.iictenterprisesllc.com/.

Mar 10, 2014 N07: Intermediate Dimensional Metrology. Long Beach CA (MSC). NIST/Office of Weights and Measures. http://www.nist.gov/pml/wmd/calendar.cfm.

Mar 10-11, 2014 Hands-On Gage Calibration and Repair Workshop. Las Vegas, NV. IICT Enterprises LLC. http://www.iictenterprisesllc.com/.

Mar 18-19, 2014 Hands-On Gage Calibration and Repair Workshop. Louisville, KY. IICT Enterprises LLC. http://www.iictenterprisesllc.com/.

Mar 20-21, 2014 Hands-On Gage Calibration and Repair Workshop. Indianapolis, IN. IICT Enterprises LLC. http://www.iictenterprisesllc.com/.

Apr 1, 2014 Dimensional Metrology: Applications and Techniques. Aurora IL. Mitutoyo Institute of Metrology. http://www.mitutoyo.com/support/mitutoyo-institute-of-metrology/.

Apr 1-2, 2014 Hands-On Gage Calibration and Repair Workshop. Houston, TX. IICT Enterprises LLC. http://www.iictenterprisesllc.com/.

Apr 3, 2014 Gage Calibration Systems and Methods. Aurora IL. Mitutoyo Institute of Metrology. http://www.mitutoyo.com/support/mitutoyo-institute-of-metrology/.

Apr 8-10, 2014 Hands-on Gage Calibration. Aurora IL. Mitutoyo Institute of Metrology. http://www.mitutoyo.com/support/mitutoyo-institute-of-metrology/.

Apr 24-25, 2014 Hands-On Gage Calibration and Repair Workshop. Portland, OR. IICT Enterprises LLC. http://www.iictenterprisesllc.com/.

Apr 28-29, 2014 Hands-On Gage Calibration and Repair Workshop. Salt Lake City, UT. IICT Enterprises LLC. http://www.iictenterprisesllc.com/.

May 1-2, 2014 Hands-On Gage Calibration and Repair Workshop. Denver, CO. IICT Enterprises LLC. http://www.iictenterprisesllc.com/.

May 6, 2014 Dimensional Metrology: Applications and Techniques. Hoover AL. Mitutoyo Institute of Metrology. http://www.mitutoyo.com/support/mitutoyo-institute-of-metrology/.

May 8, 2014 Gage Calibration Systems and Methods. Hoover AL. Mitutoyo Institute of Metrology. http://www.mitutoyo.com/support/mitutoyo-institute-of-metrology/.

May 15-16, 2014 Hands-On Gage Calibration and Repair Workshop. Rochester, NY. IICT Enterprises LLC. http://www.iictenterprisesllc.com/.

May 19-20, 2014 Hands-On Gage Calibration and Repair Workshop. Manchester, MA. IICT Enterprises LLC. http://www.iictenterprisesllc.com/.

May 20-22, 2014 Hands-on Gage Calibration. Aurora, IL. Mitutoyo Institute of Metrology. http://www.mitutoyo.com/support/mitutoyo-institute-of-metrology/.

Jun 5-6, 2014 Hands-On Gage Calibration and Repair Workshop. Schaumburg, IL. IICT Enterprises LLC. http://www.iictenterprisesllc.com/.

SEMINARS: Electrical

Apr 7-10, 2014 MET-301 Advanced Hands-on Metrology. Seattle, WA. Fluke Calibration. http://us.flukecal.com/training/courses/MET-301.

May 13-15, 2014 MET-302 Introduction to Measurement Uncertainty. Everett, WA. Fluke Calibration. http://us.flukecal.com/training/courses/MET-302.

Jun 2-5, 2014 MET-101 Basic Hands-on Metrology. Everett, WA. Fluke Calibration. http://us.flukecal.com/training/courses/MET-101.

Jun 9-12, 2014 MET-301 Advanced Hands-on Metrology. Seattle, WA. Fluke Calibration. http://us.flukecal.com/training/courses/MET-301.

SEMINARS: Flow & Pressure

Mar 10-11, 2014 N03: Flow Measurement and Uncertainties. Long Beach CA (MSC). NIST/Office of Weights and Measures. http://www.nist.gov/pml/wmd/calendar.cfm.

Mar 10-11, 2014 N02: NIST Pressure and Vacuum Measurement. Long Beach CA (MSC). NIST/Office of Weights and Measures. http://www.nist.gov/pml/wmd/calendar.cfm.

CALENDAR

Mar 25-27, 2014 European Flow Measurement Workshop: Ultrasonic & Coriolis Metering. Lisbon, Portugal. Colorado Engineering Experiment Station Inc. (CEESI) http://www.ceesi.com.

Mar 25-27, 2014 Principles and Practice of Flow Measurement Training Course. East Kilbride, UK. NEL, www.tuvnel.com.

Apr 7-11, 2014 Principles of Pressure Calibration. Phoenix, AZ. Fluke Calibration. http://us.flukecal.com/Principles-of-Pressure.

SEMINARS: General & Management

Mar 18-20, 2014 Cal Lab Management; Beyond 17025 Training. Boca Raton, FL. WorkPlace Training. http://www.wptraining.com.

Mar 31-Apr 4, 2014 Fundamentals of Metrology. Gaithersburg, MD. NIST / Office of Weights and Measures. http://www.nist.gov/pml/wmd/labmetrology/training.cfm.

May 19-22, 2014 Effective Cal Lab Management. Everett, WA. Fluke Calibration. http://us.flukecal.com/lab_management_training.

May 21-22, 2014 Laboratory Performance Improvement Using Statistical Tools. Minneapolis, MN. http://www.wptraining.com.

SEMINARS: Industry Standards

Mar 10-11, 2014 N05: The ISO/IEC 17025 Accreditation Process. Long Beach CA (MSC). NIST/Office of Weights and Measures. http://www.nist.gov/pml/wmd/calendar.cfm.

May 7-9, 2014 ISO/IEC Standard 17025 Training for Testing and Calibration Laboratories. La Habra, CA. International Accreditation Service (IAS), http://www.iasonline.org/More/training.html.

SEMINARS: Mass

Apr 28-May 9, 2014 Mass Metrology Seminar. Gaithersburg, MD. NIST / Office of Weights and Measures. http://www.nist.gov/pml/wmd/labmetrology/training.cfm.

SEMINARS: Measurement Uncertainty

Mar 3-4, 2014 Measurement Uncertainty (per ILAC P14 Guidelines). Boca Raton, FL. http://www.wptraining.com.

Mar 6, 2014 Introduction to Measurement Uncertainty Training Course. Kuala Lumpur, Malaysia. TUV SUD Ltd. http://www.tuvnel.com/tuvnel/courses_workshops_seminars/.

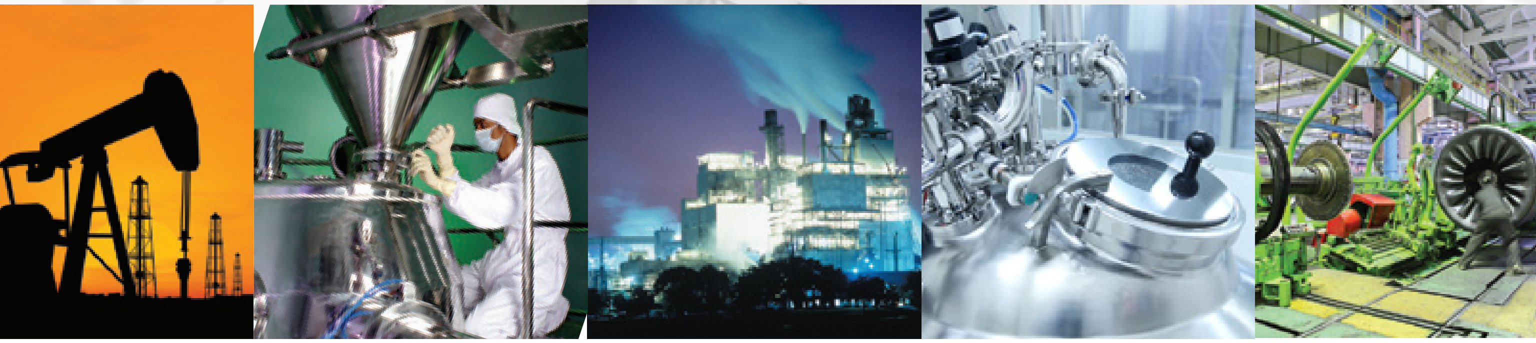

CALENDAR

Mar 10-12, 2014 N06: Hands-on Workshop, Assessing & Reporting Measurement Uncertainty. Long Beach CA (MSC). NIST/Office of Weights and Measures. http://www.nist.gov/pml/wmd/calendar.cfm.

Mar 18-19, 2014 Estimating Measurement Uncertainty. Westford, MA. Mitutoyo Institute of Metrology. http://www.mitutoyo.com/support/mitutoyo-institute-of-metrology/.

Apr 15-16, 2014 Estimating Measurement Uncertainty. Aurora IL. Mitutoyo Institute of Metrology. http://www.mitutoyo.com/support/mitutoyo-institute-of-metrology/.

May 8-9, 2014 Measurement Uncertainty (per ILAC P14 Guidelines). Dallas, TX (following the ASQ World Conf). WorkPlace Training http://www.wptraining.com.

May 27-29, 2014 Measurement Uncertainty (per ILAC P14 Guidelines). Lincoln, NE. WorkPlace Training http://www.wptraining.com.

Jun 17-18, 2014 Measurement Uncertainty (per ILAC P14 Guidelines). Boston, MA. WorkPlace Training http://www.wptraining.com.

SEMINARS: Temperature

Mar 10-12, 2014 N01: Selection, Calibration, and Use of Contact Thermometers. Long Beach CA (MSC). NIST/Office of Weights and Measures. http://www.nist.gov/pml/wmd/calendar.cfm.

May 20-22, 2014 Infrared Temperature Metrology. American Fork, UT. Fluke Calibration. http://us.flukecal.com/tempcal_training.

Jun 10-12, 2014 Principles of Temperature Metrology. American Fork, UT. Fluke Calibration. http://us.flukecal.com/training/courses/Principles-Temperature-Metrology.

SEMINARS: Vibration

Apr 8-10, 2014 Fundamentals of Random Vibration and Shock Testing. Detroit, MI. http://www.equipment-reliability.com.

Jun 3-5, 2014 Fundamentals of Random Vibration and Shock Testing. Boxborough, MA. http://www.equipment-reliability.com.

SEMINARS: Volume

Aug 18-22, 2014 Volume Seminar. Gaithersburg, MD. NIST / Office of Weights and Measures. http://www.nist.gov/pml/wmd/labmetrology/training.cfm.

INDUSTRY AND RESEARCH NEWS

Agilent Technologies Reveals Name of Electronic Measurement Spin-Off Company

Agilent Technologies Inc. revealed the name of the electronic measurement company it expects to spin off in early November 2014 as Keysight Technologies.

The name Keysight conveys the ability to see what others cannot, offering the critical or key insights to understand and unlock the changing technology landscape. The new company's tagline, "unlocking measurement insights for 75 years," commemorates the 1939 birth of the original Hewlett-Packard Company, from which Keysight originated.

"Keysight reflects our rich heritage—a direct line from both Hewlett-Packard's standards of integrity and innovation and Agilent's premier measurement business," said Ron Nersesian, president and CEO of Keysight.

"This name captures the spirit of our organization—innovative, insightful and forward-looking," said Nersesian, who added, "While Keysight is built on 'firsts' dating back to the birth of Silicon Valley, as a new company we are committed to bringing our customers a new generation of firsts—unlocking insights for them so they can in turn bring a new generation of technologies into the world."

Keysight will include the entire portfolio of Agilent electronic measurement products and the largest sales and support team in the test and measurement industry.

Expected to become a standalone company in early November 2014, Keysight will be headquartered in Santa Rosa, Calif., and have approximately 9,500 employees in 30 countries. The company's website is www.keysight.com.

On Sept. 19, 2013, Agilent announced plans to separate into two publicly traded companies through a tax-free spinoff of its electronic measurement business.

AMETEK Acquires Teseq Group

AMETEK, Inc. has acquired the Teseq Group, a leading manufacturer of test and measurement instrumentation for electromagnetic compatibility (EMC) testing, for CHF 83 million ($92 million). Headquartered in Luterbach, Switzerland, the privately held company has annual sales of approximately CHF 48 million ($53 million).

Teseq manufactures a broad line of conducted and radiated EMC compliance testing systems and RF amplifiers for a wide range of industries, including aerospace, automotive, consumer electronics, medical equipment, telecommunications and transportation.

"Teseq is an excellent addition to our electrical test and measurement business. It is a global leader in conducted and radiated EMC test equipment with a comprehensive product offering and extensive geographic coverage," comments Frank S. Hermance, AMETEK Chairman and Chief Executive Officer.

"Teseq's products and markets are complementary with our EM Test business, which we acquired in 2011. Its addition to that business provides us with opportunities for accelerating product innovation and market expansion worldwide," adds Mr. Hermance.

Teseq has manufacturing and development operations in Luterbach as well as Germany, the United Kingdom and the United States with direct sales offices in China, France, Germany, Japan, Singapore, Switzerland, Taiwan, the United Kingdom and the United States.

It joins AMETEK as part of its Electronic Instruments Group (EIG) -- a recognized leader in advanced monitoring, testing, calibrating, and display instruments with 2012 sales of $1.9 billion.

Tektronix Acquires Picosecond Pulse Labs

Tektronix, Inc., a leading worldwide provider of test, measurement and monitoring instrumentation, announced January 16, 2014, the acquisition of Picosecond Pulse Labs. The move is intended to strengthen the Tektronix portfolio in the growing market for test equipment to support 100G/400G optical data communications research and development. The terms of the transaction were not disclosed. Privately-held Picosecond Pulse Labs, based in Boulder, Colorado, offers products that include ultra-high-speed pattern generators, the world's fastest pulse generators and highest bandwidth sampler modules. The company recently introduced the PatternPro line that includes multi-channel 32 Gb/s data generators and analyzers for 100G/400G applications. "Picosecond Pulse Labs has a long history of designing and manufacturing cutting-edge instrumentation and brings a particular focus on the high-speed optical test market with its new 32 Gb/s error detectors and pattern generators," said Amir Aghdaei, president of Tektronix. "When combined with our high-speed oscilloscopes and other product offerings, Picosecond will further strengthen our portfolio of solutions in the critical 100G/400G data communications segment."

About Tektronix:

For more than sixty-five years, engineers have turned to Tektronix for test, measurement and monitoring solutions to solve design challenges, improve productivity and dramatically reduce time to market. Tektronix is a leading supplier of test equipment for engineers focused on electronic design, manufacturing, and advanced technology development. Headquartered in Beaverton, Oregon, Tektronix serves customers worldwide and offers award-winning service and support. Stay on the leading edge at www.tektronix.com.

About Picosecond:

Picosecond Pulse Labs, Inc. (PSPL) is located in Boulder, CO. Founded in 1980 by Dr. James R. Andrews, PSPL designs and manufactures instruments, modules, and components for test & measurement applications. Picosecond's core competence is the precision generation and measurement high-speed signals. A key part of this competency is our long legacy of designing metrology grade test equipment.

NIST Stars in Media's Top Science and Technology Stories of 2013

National Institute of Standards and Technology (NIST) advances in atomic clocks and telescope cameras made it into five magazines' lists of the top science and technology stories of 2013.

NIST's ytterbium lattice atomic clocks—the world's most stable clocks as of 2013—were cited in two media lists of the year's top discoveries. These experimental clocks use about 10,000 rare-earth atom strapped in a lattice of laser light to achieve high stability, which can be thought of as how precisely the duration of each tick matches every other tick. *Time* magazine's The 25 Best Inventions of the Year 2013 include, in the Totally Cool category, A New Atomic Clock. In addition, the French science magazine *La Recherche* cited advances in atomic clocks, including NIST's ytterbium clocks, as the number six discovery of the year.

A discovery by the South Pole Telescope, which relies on a camera made of NIST's superconducting sensors and amplifiers, was cited in two magazines' top 10 lists and another magazine's year in review.

Physics World's Top10 Breakthroughs of 2013 include the "first detection of a subtle twist in light from the cosmic microwave background (CMB), known as B-mode polarization." This faint signal, caused by ancient light deflecting off matter, maps the distribution of all matter in the universe. This information can be used to study the properties of dark matter, dark energy, the masses of the neutrinos and test models of the evolution of the universe. The magazine cited "improvements in detector technology" as the major reason behind the discovery. The background signal detected in 2013 will be subtracted from future observations of spatial variations in the CMB as scientists look for gravitational waves, or ripples in the fabric of space-time, that would indicate rapid early inflation of the universe.

Astronomy magazine's Top 10 Space Stories of 2013 included the South Pole Telescope's detection of B-mode polarization at number three: Advanced instruments observe the early universe. The magazine called the discovery "an important milestone in research, as it shows that scientists are digging deeper into what the CMB holds." The discovery was also mentioned in *Nature* magazine's 365 Days: 2013 in review.

Source: *NIST Tech Beat, Jan. 14th, 2014, http://www.nist.gov/public_affairs/tech-beat/tb20140114.cfm#stories.*

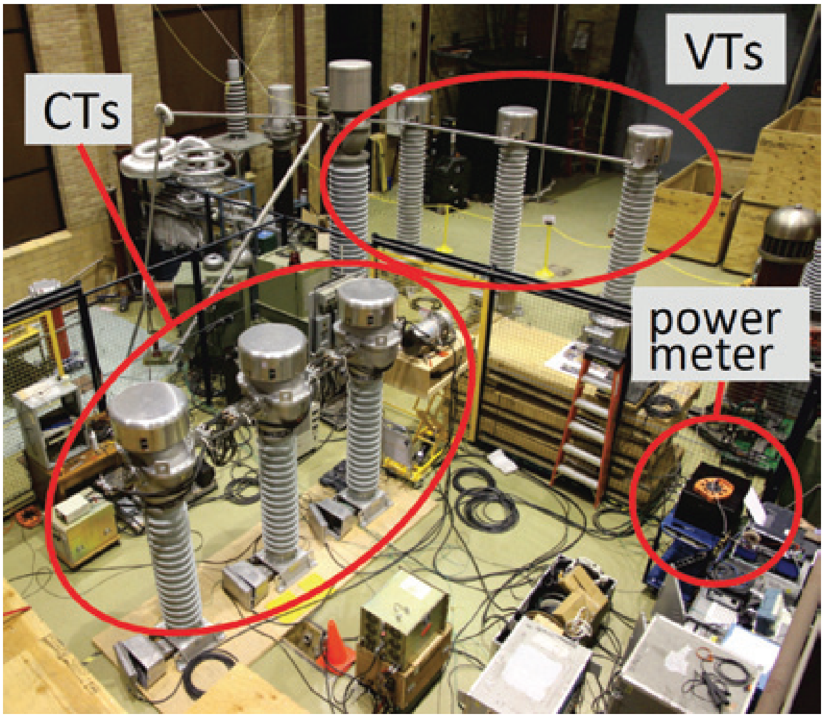

Validation of the complete VSL HV revenue metering set-up at NRC, Canada.

VSL Reference Set-up for Revenue Metering in High Voltage Power Grids (150 kV, 5 kA)

Liberalisation of the energy market and increased use of renewable energy sources has raised interests in metering of electricity flows between parties exploiting the electricity grid. Such grid metering must be performed with high accuracy since small errors correspond to large amounts of money.

Driven by the economic importance of correct revenue metering in high voltage (HV) grids, VSL has developed a reference set-up for validating existing revenue metering systems in the HV power grid. The original aim was to have an uncertainty of better than 0.1 % (1000 ppm), at least five times more accurate than existing grid revenue metering systems. The VSL reference set-up has been built up around custom-made current and voltage transformers (CTs, VTs) and a three-phase reference power/energy meter. With this set-up, power and energy can be measured in three-phase high voltage lines, at 110 kV and 150 kV, with currents up to 5 kA.

After calibration of the individual components in the VSL reference system, an overall validation was performed at NRC, Canada (see photograph). Whereas an agreement of around 100 ppm was expected, the actual agreement between the VSL and NRC systems was really excellent: better than 25 ppm at a power level of 200 MW. Based on these results, a VSL system uncertainty of better than 300 ppm is estimated for actual on-site measurements – three times better than the original aim.

At the end of 2013, the VSL system will be completely ready for on-site measurements. This is just in time for power plant owners and large electricity consumers in the heavy industry that have already contacted VSL for on-site verification of their revenue metering systems.

Contact Martin Fransen (mfransen@vsl.nl) or Gert Rietveld (grietveld@vsl.nl) for more information on this subject.

NIST Programs for Undergraduates, Teachers, Precision Measurements Announced

The National Institute of Standards and Technology (NIST) is advertising available grants in a pair of programs aimed at undergraduate students and middle school teachers, as well as the latest round of the agency's long-running Precision Measurement Grants program. All three were recently announced at the federal funding web site Grants.gov.

The NIST Summer Undergraduate Research Fellowship (SURF) program provides an opportunity for undergraduate students to spend a summer working with the internationally recognized NIST research staff on projects in a wide variety of disciplines at either the main NIST laboratories in Gaithersburg, Md., or its laboratories in Boulder, Colo. Applications are made on behalf of the students by their academic institutions. Applications must be received by Feb. 14, 2014. Full details of the program, rules and the application process are available at Grants.gov under funding opportunity2014-NIST-SURF-01. See www.grants.gov/web/grants/view-opportunity.html?oppId=248933.

The NIST Summer Institute for Middle School Science Teachers program is a two-week workshop at NIST's Gaithersburg, Md., campus combining lectures, tours and hands-on activities that educators can recreate in their own classrooms. The program aims to increase teachers' understanding of the subjects they teach, provide materials and resources to implement what they have learned at NIST in the classroom, enhance their enthusiasm for science, increase teachers' understanding of how scientific research is carried out and provide them with the opportunity to develop an ongoing network of scientists and engineers at NIST who will be available for consultation even after the NIST Summer Institute program has ended.

Public school districts or accredited private educational institutes in the United States and/or its territories that offer general science classes at grade levels 6-8 are eligible to nominate teachers to participate. Individual teachers do not apply directly, but through their schools or school districts. Applications must be received by March. 12, 2014. Full details of the program, rules and the application process are available at Grants.gov under funding opportunity 2014-NIST-SUMMER-INSTITUTE-0. See www.grants.gov/web/grants/view-opportunity.html?oppId=249056.

Since 1970, NIST has sponsored its Precision Measurement Grants Program (PMGP). Awarded primarily to researchers at universities and colleges, the grants enable them to conduct significant research in the field of fundamental measurement or the determination of more precise values for fundamental constants of nature. NIST sponsors these research projects primarily to encourage basic, measurement-related research in universities and colleges and other research laboratories. The PMGP also is intended to make it possible for researchers to pursue new ideas in measurement science for which other sources of support may be difficult to find.

NIST anticipates funding two projects at most, depending on the availability of funding, for up to three years at $50,000 per year. Eligible proposers are accredited institutions of higher education; hospitals; nonprofit organizations; commercial organizations; state, local and Indian tribal governments; foreign governments; organizations under the jurisdiction of foreign governments; international organizations; and federal agencies with appropriate legal authority. Applications must be received by May 6, 2014. Full details of the program, rules and the application process are available at Grants.gov under funding opportunity 2014-NIST-PMGP-01. See www.grants.gov/web/grants/view-opportunity.html?oppId=248854.

Source: *NIST TechBeat, Dec 17, 2013, http://www.nist.gov/public_affairs/tech-beat/tb20131217.cfm#grants.*

A commercial high-precision calibrator (center) is calibrated by means of the AC quantum voltmeter in the AC voltage mode.

AC Quantum Voltmeter for Industry

Within the scope of a technology transfer project involving PTB and two partners from industry, which was supported by the Federal Ministry of Economics and Technology, a Josephson measuring system for DC and AC voltages – an AC quantum voltmeter – has been developed for use in industrial calibration laboratories. With this new system, the considerable advantages of electrical standards based on quantum effects will also become available to industrial laboratories: very low measurement uncertainties are possible without tedious re-calibrations, which have thus become more economical.

The system is based on Josephson arrays, which are manufactured at PTB, and is designed for peak voltages of up to ± 10 V and frequencies of up to 10 kHz. With a prototype, AC voltages from 10 Hz to 4 kHz have already been measured at PTB, whereby uncertainties of a few µV/V within a measuring time of one minute were attained. This makes the new AC quantum voltmeter approximately 20 times more accurate than conventional calibrators and 60 times faster than the measurement procedures with thermal converters used to date.

In addition, the AC quantum voltmeter can also calibrate commercial DC voltage standards (DC references and DC voltmeters) and, thus, also covers the range of commercially available DC quantum voltmeters. During a direct 10 V comparison between a DC quantum voltmeter and the new AC prototype, no significant deviation was observed within a measuring time of 15 minutes within the uncertainty limit of 0.1 nV/V.

The new AC quantum voltmeter is now being optimized by means of on-site tests at the partner's (esz AG) accredited laboratory. With this valuable end-user input, it will be developed to become a fully automated, user-friendly measuring system. The main objective is to reach a relative uncertainty of 2.5 µV/V at 1 kHz. The system will be developed in a modular approach which will allow a future extension of the system to a universal "quantum calibrator" for voltage, resistance and current standards. Supracon AG (instrument manufacturer), the other project partner, will be in charge of the subsequent marketing.

Source: *PTBNews Issue 2:2013 (English Version), http://www.ptb.de/cms/en/publikationen/zeitschriften/ptb-news/ptb-news-2013-2/ac-quantum-voltmeter-for-industry.html.*

Keithley Low Level Measurements Handbook, 7th Ed. Release

Keithley Instruments, Inc., a world leader in advanced electrical test instruments and systems, announced today that it has published the seventh edition of its well-regarded Low Level Measurements Handbook: Precision DC Current, Voltage, and Resistance Measurements. This 250-page reference, which Keithley first published in 1972, describes theoretical and practical considerations involved in the measurement of low DC currents, high resistances, low DC voltages, and low resistances. Among other updates, the seventh edition incorporates information on the latest electrical measurement tools and techniques, including those developed for characterizing today's nanoscale devices and high power semiconductors. The handbook can be downloaded at no cost at http://www.keithley.com/promo/wb/1401.

Section 1 offers an overview of the expanding range of low level DC measuring instruments now available to scientists and engineers, including the electrometer, digital multimeter (DMM), nanovoltmeter, picoammeter, source measure unit (SMU) instrument, low current preamp, micro-ohmmeter, and low current source. Sections 2 and 3 delve into techniques and sources of error related to measurements from high resistance and low resistance sources respectively. Both sections include a measurement optimization summary that allows readers to identify likely sources of measurement error and troubleshooting techniques at a glance. Section 4 provides useful information on configuring test setups for a wide range of low level measurement applications.

The handbook concludes with an updated instrument selection guide, an illustrated cable and connector assembly guide, glossary, and test system safety reference. A detailed index helps readers find specific topics quickly.

Agilent Technologies USB Thermocouple Power Sensors

Agilent Technologies Inc. announced the addition of two new models to its U8480 Series USB thermocouple power sensors. The U8480 Series now comes with improved specifications, including an expanded frequency range to 67 GHz and a measurement speed of 900 readings/second, maintaining the U8480 Series' status as the world's fastest USB thermocouple power sensors.

The U8480 Series' real-time measurement uncertainty feature significantly reduces overall test time by removing the need for time-consuming manual measurement uncertainty (MU) calculations. Users can now compute MU in real time and at any given point. The feature also allows them to display power measurements and their MU simultaneously, simplifying test measurement and increasing test accuracy.

The U8480 Series provides best accuracy and repeatability with thermocouple sensing technology and a power linearity of less than 0.8 percent. The new S-parameter and gamma correction functions further improve measurement accuracy by correcting the mismatch errors caused by inserted components between the device-under-test and the power sensor, making the U8480 Series suitable for applications such as test system or instrument calibration.

Like all Agilent USB power sensors, the U8480 Series can be used as an accessory for other Agilent instruments, allowing these instruments to perform specific power measurement applications without needing to connect to a PC or laptop. The U8480 Series is compatible with Agilent FieldFox RF analyzers and MXG signal generators, giving them power meter functionalities. The power sensors also perform source power calibration with Agilent PNA, PNA-L and PNA-X network analyzers. And with USB functionality and the bundled N1918A Power Panel software, measuring high-frequency power measurements in applications ranging from high-volume manufacturing to calibration and field remote monitoring has never been more convenient.

Information on the U8480 Series is available at www.agilent.com/find/usbthermosensor_pr. Visit the Power Meter and Sensor channel on the Agilent YouTube network at www.youtube.com/Agilentpwrmetersensr to see the latest videos related to Agilent's power-meter and sensor family.

Fairview Microwave Variable RF Switch Attenuators

Fairview Microwave, Inc. a preeminent supplier of on-demand microwave and RF components, has released a new line of compact hot-switchable variable attenuators. RF attenuators are used to reduce the amplitude of an electronic signature in many common electronic scenarios including lab testing equipment, distributed antenna systems (DAS) and power and signal monitoring systems.

Fairview Microwave's new line of variable step attenuators come in 3 and 6 GHz frequency models and several different connector configurations including SMA and N type connectors with side or rear mount positions. Several of these attenuators are hot-switchable, meaning attenuation can be changed on the fly without powering down the system, allowing test data to be read continuously. Several models with varying attenuation adjustments are available including 0 to 12 dB attenuation in 1 dB steps and 0 to 40 dB attenuation in 10 dB steps, with other options available upon request.

These new attenuator products also boast low attenuation tolerance and low insertion loss. "Our new lines of hot-switchable variable attenuators provide engineers the flexibility to adjust and customize the RF performance of their distributed systems while the system is live", says Greg Arnold, Technical Sales Manager for Fairview Microwave. "This adds an invaluable tool to the arsenal of components available to engineers for efficiently optimizing their DAS, multi-element antenna arrays or any multi-channel system requiring individual amplitude adjustment."

Fairview's new hot-switchable variable attenuators are in-stock and available to ship today. You can view the complete offering of RF coaxial attenuators from Fairview Microwave by visiting http://www.fairviewmicrowave.com/coaxial_attenuators.htm. For additional information, Fairview can be contacted at +1-972-649-6678.

A leading supplier of on-demand RF and microwave products since 1992, Fairview Microwave offers immediate delivery of RF components including attenuators, adapters, coaxial cable assemblies, connectors, terminations and much more. All products are shipped same-day from the company's ISO 9001:2008 certified production facilities in Allen, Texas.

Rohde & Schwarz FSW-B500 Option

The new R&S FSW-B500 hardware option is now available for all analyzers of the R&S FSW family and can therefore be used for measurements in a frequency range up to 67 GHz. This enables completely new applications for the signal and spectrum analyzer in research and development. The analyzer is especially well-suited for sophisticated measurement tasks in radar or satellite applications as well as for tests on fast wireless connections such as WLAN or Beyond 4G (5G).

The large analysis bandwidth enables users to test pulse rise and fall times from approximately 3 ns or very short pulses from an 8 ns pulse width. The analyzer can therefore be used in the development of radar systems for automotive applications, for example. Users can fully record and measure radar chirps with up to 500 MHz bandwidth. Hopping sequences in frequency-agile communications systems such as tactical radios can also be easily analyzed. Researchers working on satellite applications will be able to characterize the components for the future transponder generation with up to 500 MHz analysis bandwidth. Components for microwave links can also be measured with up to 500 MHz bandwidth.

The R&S FSW now offers developers of RF amplifiers for mobile radio or WLAN the ability to measure digital predistortion of amplifiers with up to 160 MHz bandwidth, as required for WLAN 802.11ac signals, for example. In the past, measuring these kinds of wideband signals often required complicated setups consisting of a digital oscilloscope and a downconverter.

The R&S FSW-B500 option for the R&S FSW high-end signal and spectrum analyzer is now available from Rohde & Schwarz. Internet: www.rohde-schwarz.com.

NEW PRODUCTS AND SERVICES

Yokogawa PX8000 Precision Power Scope

Yokogawa has combined its world-leading expertise in power measurement and its long heritage in oscilloscope design to create the world's first Precision Power Scope: the Model PX8000.

The PX8000 brings oscilloscope-style, time-based measurement to the world of power measurement. It can capture voltage and current waveforms precisely, opening up applications and solutions for a huge variety of emerging power measurement problems.

The new instrument has 12-bit resolution with 100 MS/s sampling and 20MHz bandwidth. This means that the PX8000 can be used for accurate measurement of inverter pulse shapes, which can then be used to fine-tune inverter efficiency. A choice of input modules covers voltage, current and sensor measurements at voltages up to 1000 V RMS and currents up to 5 A RMS, with a basic accuracy of ±0.1%. Higher currents can be measured with external current sensors. The PX8000 can be configured to evaluate single phase and three-phase electrical systems.

In addition to delivering precision power measurement to give true insight into energy consumption and performance, the PX8000 incorporates a number of innovative features that support the crucial measurement and analysis of transient power profiles. It provides simultaneous voltage and current multiplication to give real-time power sampling, supporting both transient measurement (as standard) and numerical values averaged across the sample period. Up to 16 different waveforms – including voltage, current and power – can be displayed side-by-side, giving engineers instant "snapshots" of performance.

A variety of functions including arithmetical calculations, time shifting and Fast Fourier Transforms enables users to display waveforms with offsets and skew corrections. An automatic de-skewing function eliminates offsets between current and voltage signals that may be caused by sensor or input characteristics. Users can also define their own computations via equations that combine differentials, integrals, digital filters and other functions.

Applications for the PX8000 cover everything from sustainable power to advanced robotics. Any situation where power consumption is at a premium can benefit from the introduction of the PX8000's precision measurement and analysis capabilities. Typical application sectors include inverter and motor testing, reactor loss measurement of inverter boost circuits, transient responses of industrial robots, wireless charger efficiency measurement, and voltage and power measurements in electricity distribution systems.

For further information about the PX8000 visit www.tmi.yokogawa.com.

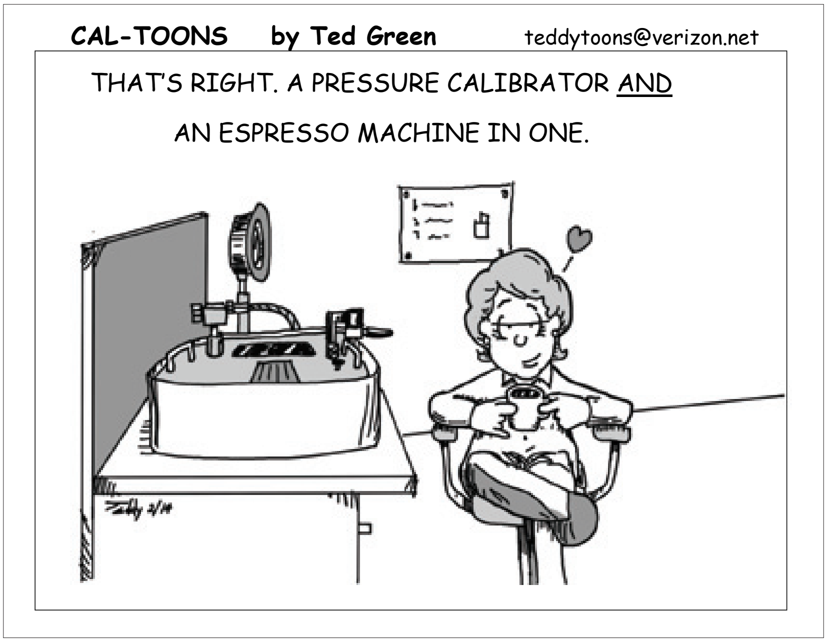

Laboratory Quality/Management: A Workbook with an Eye on Accreditation

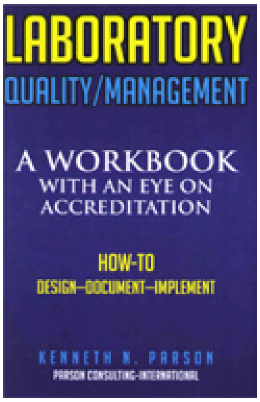

To develop, document, and implement a well-designed management system for laboratories is one of the most difficult and frustrating activities that can be undertaken by management. There has not been much information available on how one might approach such an effort.

This book, by Kenneth N. Parson, should be of interest to the management of all types of laboratories supporting all types of scientific disciplines. The book addresses principal elements of laboratory management, technical and support operations, and offers several detailed "how to" procedures designed to help laboratory management to establish and maintain control through a continuous low level internal audit, (self assessment) process. This activity enables management to take prompt corrective action, maintain control and provides the ability to measure improvement over time toward achieving a higher level of quality services to its assigned customers.

The objective of this book is to expand on the knowledge and understanding of laboratory quality/management system process. It should be helpful to those laboratories considering accreditation, those accredited, and those simply interested in improving on their management processes and methods of operation.

Available in hardback, softcover, or as ebook: www.xlibris.com, www.amazon.com, www.bn.com, or visit your local bookstore.

Measurement Specialties' Miniature Pressure Sensor

Measurement Specialties (NASDAQ: MEAS), an expert in sensor design and manufacturing, has released the rugged XP5, a miniature pressure sensor with SanShift technology that eliminates zero shifts caused by installation torque.

Designed for use in environments involving measurements in corrosive liquids and gases, as found in automotive, military and aerospace applications, as well as for rugged onboard equipment monitoring, the XP5 features a body and flush diaphragm constructed of titanium and is laser welded for increased durability.

A temperature-compensated Wheatstone bridge with high stability micro-machined silicon strain gauges makes up the core sensing technology of the new sensor. This enables the user to select various levels depending upon available options.

The XP5 can be used in both static and dynamic applications, and is available in absolute, sealed and gauge configurations from 1 bar to 70 bar, with a sealed format available up to 350 bar.

Several options, including an onboard amplifier for ranges from 5 bar to 350 bar as well as a custom temperature probe for all ranges, provide design flexibility and sensor customization to fit specific application requirements.

The IP50-rated XP5 conforms to EN 61010-1, EN 50081-1 and EN 50082-1. Frequency response in a non-amplified XP5 ranges from 108 kHz to 700 kHz. In addition, IP67 and IP68 versions are available upon request.

Technical Specifications:

- Linearity to ±0.25% FSO from 5 bar to 350 bar; ±0.5% FSO for lower ranges
- M5x0.8 or 10-32UNF-2A thread screw mounting; specific lengths on request
- Operating temperature: -40°C to 120°C
- Compensated temperature: 0°C - 60°C

For more information, visit http://www.meas-spec.com/product/tm_product.aspx?id=10043.

Picosecond 40Gb/s BERT System

Picosecond announces the industry's first 40Gb/s BERT with jitter insertion, a built-in clock source, and a programmable error detector. The system creates stressed receiver test signals, measures BER, produces bathtub curves, and performs contour analysis. Picosecond Pulse Labs' 40Gb/s NRZ BERT system incorporates the SDG Model 12080 programmable pattern generator and the SDA Model 13030 programmable error detector.

While each pattern generator or error checker is a fully integrated, bench-top instrument, having separate instruments for PG and ED functions offers a great deal of flexibility that improves equipment utilization and lowers cost.

PSPL's line of PatternPro serial data test instruments enables testing of the latest NRZ and PAM-4 high-speed serial data standards by addressing critical configuration and cost issues.

The PatternPro line includes SDG Pattern Generators, SDA Error Detectors, and analysis software that provide high-performance, flexible Bit Error Test solutions. With PatternPro test suites, users are finally able to comprehensively test critical multi-channel product performance parameters such as multi-channel functionality, receiver stress testing, and victim-aggressor analysis. For more info visit: www.picosecond.com.

Tolerances for Non-Linear Analog Resistance Scales

Thomas Morgan

A method is derived for calculating the resistance tolerances for non-linear resistance scales, whose accuracy tolerances are given in degrees of arc instead of percent of reading or range.

Introduction

Back in the day, the instrument most universally used by technicians in the field and on the bench was the Volt-Ohm-Milliammeter, or V-O-M. It was portable, had a black plastic case, and large easy to read analog scales. Two of the most popular models were the Simpson 260 and the Triplett 630. They have been produced in various versions for decades and legions of faithful fans still swear by them.

But this is ancient history you say. Why would anybody be concerned with those museum pieces? Well through 30 years of working in Metrology labs I have noticed 3 things:

- The meters are still in use. I have seen a pallet of new meters being prepared for shipment. They still show up in cal lab receiving bays, even if they sometimes generate smiles and jokes.
- Different labs have different methods of interpreting the resistance accuracy specs, which are given in degrees instead of percent.
- Many technicians believe, or know some veteran tech who believes, that you can learn things troubleshooting with an analog meter that you just can't using a digital meter.

So the meters are still out there, and still need calibrating. The voltage and current functions are straightforward enough, with tolerances listed in percentages. But what to do with that darn backwards reading non-linear resistance scale with a tolerance given in degrees of arc?

Well it turns out that with a little geometry and algebra those degrees of arc can be turned into minimum and maximum resistance values. The process explained here is based on the Simpson 260 meter but the concept can be applied to other models.

Figure 1. Meter face of the Simpson 260. Picture courtesy of simpson260.com.

Reference Material

Examining the meter face (Figure 1) reveals a few interesting facts:

- The resistance scale reads backwards compared to the AC and DC scales. Zero is on the right and full scale is on the left.
- The resistance scale is highly non-linear. The length of scale equal to one Ohm on the low end covers hundreds of Ohms on the high end.
- The value of 12 Ohms lines up exactly with the midpoint of the DC scale. This corresponds to the statement in the manual that 12 Ohms is mid-scale. This value is important for the tolerance calculations.
- The full scale arc of the resistance scale is 100°. That is the value measured on a meter using a protractor. The image in Figure 1 may have been skewed by software and measure a different angle. This value is also used in the calculations.
- The 0 - 250 DC scale is linear, has 50 minor divisions and is right below the nonlinear resistance scale. Its end points line up with the resistance scale, so it also spans 100°. This turns out to be useful as will be seen below.

Specifications

Here are the resistance accuracy specifications for the Simpson 260:

Series	Range	Tolerance
1,2	All	Not specified
3	All	3°
4-9	R x 1	2.5°
	R x 100, 10k	2°

Equations

This example will be based on the R x 1 scale of a series 4 through 9 meter.

The R x 1 scale uses a 1.5V 'D' cell for power. The meter is considered as a Thevenin equivalent DC circuit with an open circuit voltage (V_{oc}) of 1.5 and an internal resistance of 12 Ω. This is because the mid-scale reading of 12 Ω occurs when internal resistance (R_{int}) = external resistance R. Short circuit (full scale) current (I_{sc}) is thus defined as:

$$I_{sc} = V_{oc} / R_{int} = 1.5 / 12 = 0.125\text{A} \quad (1)$$

The test current when measuring any resistance R is:

$$I = 1.5 / (12 + R). \quad (2)$$

Note that Eq. 1 is a special case of Eq. 2 with R = 0 (short circuit).

Remember that the resistance scale is non-linear but the DC current and voltage scales are linear. If you look at the 0 – 250 DC scale and divide the numbers by 2 then you have a test current scale for the R x 1 scale that reads in mA. The meter deflects linearly from 0 to 100° of arc as the test current goes 0 to 125 mA. The change in current that causes 1° of deflection is:

$$125 \text{ mA} / 100° = 1.25 \text{ mA / degree} \quad (3)$$

The test current corresponding to the 2.5° tolerance is then:

$$2.5° \times (1.25 \text{ mA}/°) = 3.125 \text{ mA} \quad (4)$$

Finally rearrange Eq. 2 to solve for R so we can calculate the R at any test current I:

$$R = (1.5 / I) – 12 \quad (5)$$

Calculations

We now have what we need to calculate the upper and lower tolerances for any nominal resistance on the R x 1 scale of a Simpson 260 Series 4-9. These steps should work for other models, using the appropriate values for V_{oc}, I_{sc}, R_{int} and the tolerances:

1. Choose a test point. For the R x 1 scale let's use 10 Ω. It's a nice round number and close to mid-scale.
2. Use Eq. 2 to find the test current for the nominal resistance:
   $$I = 1.5 / (12 + 10) = 68.182 \text{ mA}$$
3. Add and subtract 3.125 mA to the nominal test current to get I high and I low:
   $$I \text{ high} = 68.182 + 3.125 = 71.307 \text{ mA}$$
   $$I \text{ low} = 68.182 – 3.125 = 65.057 \text{ mA}$$
4. Use Eq. 5 to turn I low and I high into R high and R low, respectively:
   $$R \text{ high} = (1.5 / 0.065057) – 12 = 11.057$$
   $$R \text{ low} = (1.5 / 0.071307) – 12 = 9.036$$

Note that the tolerances are not symmetrical, due to the non-linear scale. The tolerances at 10 Ω correspond to approximately +10.6% and – 9.6%. These percentages get larger as the measured value gets further away from mid-scale. Measuring 100 Ω on the R x 1 scale results in an accuracy of +34% and -21%.

Comparing the Resistance Scale and the 0 – 250 DC Scale

It was already pointed out that 12 Ω is the internal resistance and the mid-scale reading. Looking at the picture of the meter face there are other points where a value on the resistance scale appears to line up with a value on the linear DC scale. These values are predicted by Eq. 2 if you use 1500 mV for V_{oc} and double it because the DC scale goes to 250, not 125. The equation I = 3000 / (12 + R) predicts the following pairs:

R (Ω)	0	3	8	12	18	28
I x 2 (mA)	250	200	150	125	100	75

Simpson 260 Resistance Specs

Series 4 - 9

Range R X __	Tolerance degrees arc	Int. Res. Ω	V o.c. VDC	I s.c. ADC	Use Range Ω
1	2.5	12	1.5	0.125	0-200
100	2.0	1.2k	1.5	1.25m	200-20k
10k	2.0	120k	9	75μ	>20k

Range	Nominal	I nom	I low	I high	R low	R high	Accuracy, %RDG		
	Ω		mA		Ω		Low	High	Average
R X 1	1	115.38	118.51	112.26	0.66	1.36	34.3	36.2	35.2
	2	107.14	110.27	104.02	1.60	2.42	19.8	21.0	20.4
	5	88.24	91.36	85.11	4.42	5.62	11.6	12.5	12.1
	10	68.18	71.31	65.06	9.04	11.06	9.6	10.6	10.1
	20	46.88	50.00	43.75	18.00	22.29	10.0	11.4	10.7
	50	24.19	27.32	21.07	42.91	59.20	14.2	18.4	16.3
	100	13.39	16.52	10.27	78.81	134.09	21.2	34.1	27.6
Enter	200	7.08	10.20	3.95	135.05	367.70	32.5	83.9	58.2
Value>>									

Figure 2. Screenshot of Microsoft Excel™ spreadsheet with calculations.

The fact that these values do indeed line up on the meter helps validate our assumptions and calculations.

The linearity of the 0 – 250 DC scale can also be useful in testing. It has 50 minor divisions so each covers 2° of arc. On the R x 100 and 10 k scales 2° is the tolerance. If you measure 300 Ω on the R x 100 scale the tolerance calculates out to be 263.4 to 338.5 Ω. Wouldn't it be easier to simply see if it reads between 195 and 205 on the 0 – 250 DC scale? Those values have marks and we have shown it to be the same range. The same could be done for all values in the above chart, giving a pretty good linearity check (of a nonlinear scale!).

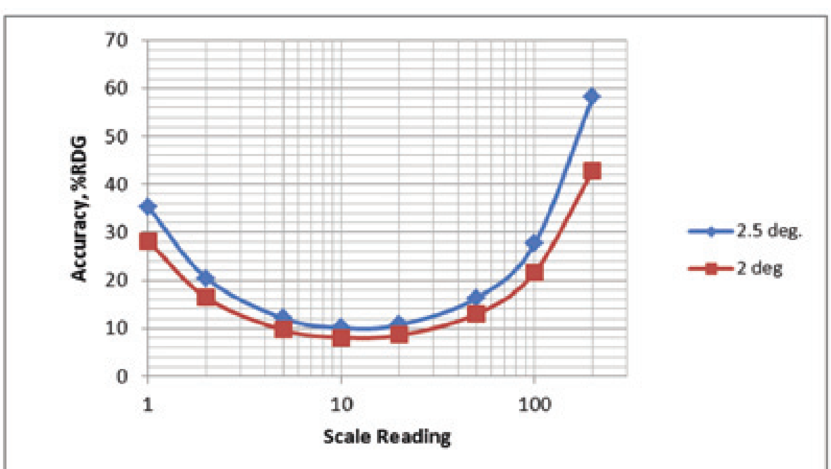

Figure 3. Chart of the average %RDG accuracy from the above table.

Automation

That was a long way to go to come up with the high and low tolerances for one test point. A process with this many equations and calculation steps naturally begs to be turned into a spreadsheet. The only math used here is simple algebra that Microsoft Excel™ or any other spreadsheet can easily handle (Figure 2).

Figure 3 is a chart of the average %RDG accuracy from the above table.

Best accuracy is mid-scale and is about 8% for the 2° tolerance and 10% for the 2.5° tolerance. It is obvious these meters are not going to be used for selecting precision resistors. But as stated above, they are out there, they need calibrating, and now you finally know how to determine their resistance tolerances.

Thomas Morgan was most recently a Metrology Engineer for Southern California Edison. He can be reached at: tjmorgan58@cox.net.

Progress in the Theory of the Laminar Tube Thermal Flow Sensor

Thomas O. Maginnis, Ph.D.

Thermal mass flow sensing is well established commercially for measurement and control of low gas flows in the semiconductor industry and elsewhere. Yet the basic theory of this critical flow sensing technology still remains poorly developed. The theoretical expression used to compute the gas correction factors is based on P.M.S. Blackett's 1930 hypothesis that the sensor response in the linear range should depend only on the heat capacity per unit time flowing through the sensor tube, and be otherwise independent of gas properties. However, this 80 year old suggestion has never been decisively proved or disproved from the theory of the sensor for real sensor designs, and its justification remains purely empirical.

The author has discovered a class of closed form exact solutions to the governing differential equations for this kind of sensor. Though these exact solutions unfortunately do not include the most common commercial sensor design, they still provide considerable insight into the physics of these sensors, and the exact solutions can be used to test Blackett's hypothesis directly for these special cases. For these simple special cases the low flow sensor slope can be evaluated exactly in closed form. These special solutions can therefore be used to provide estimates and bounds for the low flow slope in real commercial sensors. They can also be used to begin the kind of fundamental uncertainty analysis needed to assess the potential of the capillary tube thermal flow sensing technology for future development as a low flow primary mass flow standard.

Introduction

Mass flow controllers and meters based on the laminar flow thermal sensor tube have become well established as a practical commercial product indispensable to the modern semiconductor industry, and are increasingly used in the wider industrial flow market. Yet this flow technology is unique because no theoretical explanation of the sensor operation adequate for modern sensor design has ever been published.

In part this is attributable to the fact that the promise of laminar thermal flow sensor technology was largely ignored for 35 years, until it proved useful to the expanding semiconductor industry and came into heavy demand, so that the commercial exploitation of the technology occurred before its working principles were properly understood. Once the technology became commercially profitable, there was increasing demand by large users for standardization of the instrument dimensions across manufacturers. The result was premature freezing of the instrument designs by large manufacturers, so that today laminar flow thermal sensor design is in an artificially arrested state of development.

These devices basically use a heated tube to force a fluid to flow up and down a temperature hill that has mirror symmetry about the tube mid-length point. The heat capacity of the flowing fluid makes the fluid temperature lag behind the temperature of the immediately adjacent tube wall, and that temperature difference causes heat to be exchanged between the fluid and the wall. This results in a wall temperature shift that is opposite in sign for the rising and falling slopes of the temperature hill, and is directly proportional to the product of fluid mass flow rate and fluid specific heat capacity. Because the wall temperature shifts are measured from the outside of the tube, this sensing method is inherently non-invasive and can meter many corrosive and hazardous fluids. It should be noted that this sensing technique has been applied to date only to laminar flows, and primarily to gas flows, though it has also been used successfully with laminar flows of liquids.

Empirically developed modern laminar flow sensors work well for nearly ideal gases over linear flow ranges of 10 or 20 to 1, and the flow meters and flow controllers designed around them perform well and sell well. Some self-appointed experts even claim the technology is mature. Yet there is not yet an accepted, developed theory of the sensor operation available in the public domain. It is therefore not easy for a flow technologist to assess whether the present performance represents closer to 98% of the theoretically achievable performance, or only 2%. A working theory of operation is needed for the proper scientific assessment and future development of this flow technique. The commercial expansion of this dominant low flow gas measurement technology to the closely analogous case of laminar liquid flows has lagged due to the lack of availability of a reliable theory to guide design of laminar flow thermal sensors suitable for use with liquids.

The gas correction factors universally used to relate flow responses of different gases on the same instrument are based on a plausible hypothesis[1] by P.M.S. Blackett, et. al. [1] that has never been rigorously proved from theory for modern sensor designs. This is astonishing when we remember that Blackett's hypothesis was first advanced more than 80 years ago. Ample empirical confirmation that Blackett's hypothesis is at least approximately valid for the linear range of sensor response has led to its widespread use, despite this lack of theoretical justification. However, the inability of different manufactures to agree on their empirically determined gas correction factors [2] suggests the possibility that Blackett's hypothesis is only approximately valid, with the true gas correction factors being appreciably influenced by the specific details of the sensor design.

This paper will present the basic equations needed to find the steady-state temperature distributions along the sensor length as a function of mass flow, and discuss a number of exact particular solutions to them recently found that shed some light on the validity of the Blackett hypothesis. Some examples of advanced sensor designs that seek to create specific temperature profiles along the tube length to improve sensor performance will then be presented.

1 Blackett's hypothesis is that the response of a laminar thermal sensor tube in the linear portion of its flow range is directly proportional to the fluid heat capacity per unit time passing through the tube, and is otherwise independent of the fluid properties. In consequence, all fluids yield the same linear sensor response plot when sensor output is plotted against heat capacity per unit time, at flows low enough to keep the sensor output linear for each fluid.

Some History of the Method

The earliest laminar tube thermal sensor known to the author was designed and built by P.M.S.Blackett and his co-workers at the Physical Chemistry Lab in Cambridge, in 1930 [1]. They were looking for a good method to measure the relative heat capacities of gases at elevated temperatures. They based their sensor design on an approximate theoretical model that they believed captured the basic behavior of the system well enough to serve for prototype design. Their straight iron sensor tube was uniformly heated over its full length by passing constant amplitude, low frequency AC current through the tube length; the heating source was the distributed Joule dissipation occurring in the electrical resistance of the metal tube wall. At the outer ends the tube was physically clamped to a cylindrical copper temperature reservoir maintained at room temperature, which also surrounded the sensing tube, and an insulating layer of still air. The result was a tube temperature distribution along the tube length that looked much like an inverted letter U, symmetrical (at zero flow) with a maximum at the midpoint of the tube length. They employed two symmetrically placed small thermocouples as point temperature sensors to detect the flow-induced asymmetry in the axial tube temperature distribution produced by the gas flow. The flow sensing thermocouples were located at about 62% of the way from the center to the ends of the tube, well away from the end effects produced by the thermal clamps that kept the tube ends at room temperature. See Figure 1 below.

Blackett's theory, based on a second-order differential equation for the tube temperature, as loaded thermally by the flowing gas, was valid only for infinitesimal gas flows, and for the special case of a tube uniformly heated over its full length (and clamped to thermal ground at the ends). One

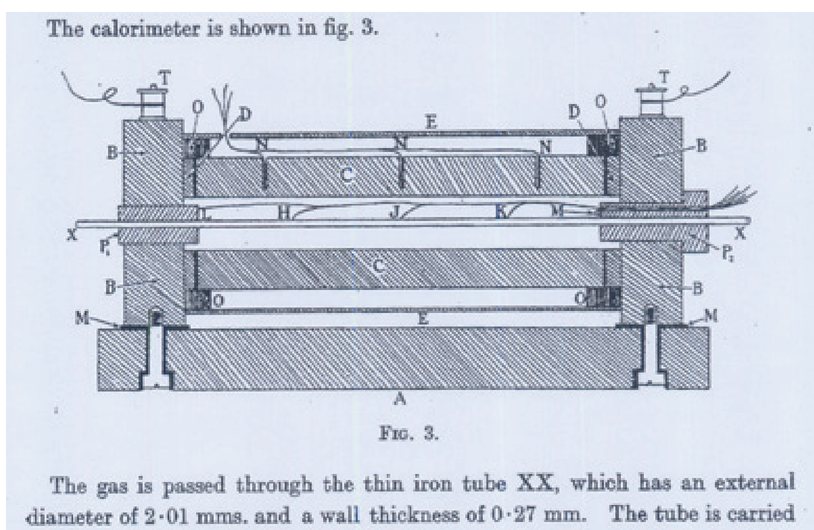

Figure 1. Cross-section of Blackett Sensor (1930). Details given below.

Tube: iron, 11.31 cm long, 2.01 mm OD, wall 0.27 mm
Case: thick copper inner, thin copper outer, separated by air insulating layers
Heating: 90 hz AC current(4 amps) passed through the iron tube, quasi-uniform
Detection: point thermocouples at H,K (spot-welded constantan) at x= +/-3.51 cm
Max linear flow (air): 30 cc/min
Estimated spec. as flowmeter: 1/4 % accuracy over range 6-60 cc/min
Thermal grounding: axial and radial, thick solid copper for uniform temperature

of his simplifying assumptions was that the axial temperature gradient in the fluid was identical to the tube axial temperature gradient at the same axial location. He states that this assumption cannot be true at the sensor ends where the tube is thermally clamped to the case.

The theory of Blackett's group was independently tested 57 years later, by Komiya et. al. [3], who used a similar experimental arrangement, but with a stainless steel tube, again with point temperature sensors at symmetrical locations relative to the tube mid-length, and again with uniform Joule effect heating of the tube along its length, and the ends clamped to a low temperature case that served as thermal ground. They reported good agreement with the Blackett theory at low flows for three gases, but substantial disagreement at higher flows. Their data with the different gases tended to confirm Blackett's hypothesis, even in the non-linear high flow portion of the flow sensor response.

Modern thermal sensor tubes do not follow the Blackett design, and his approximate theory is not correct for them. What most modern thermal sensor tubes have in common is the method of heating the sensor tube. For this one or more finite length external windings of high resistivity, high temperature coefficient insulated wire are used as electric heaters. These windings are wound on the outside surface of the sensor tube, with adjacent turns as close as practical, and the windings separated by lengths of unheated bare tube. The most common design involves two such equal and symmetrical windings, separated by a gap that is small compared to the length of tube covered by the windings, with some length of unheated tube between the outer ends of the windings and the locations where the tube is clamped to the thermal ground. When configured in an appropriate bridge circuit, and excited by a common DC current, two such adjacent windings can serve simultaneously both as tube heaters and as tube temperature asymmetry detectors. The tube is symmetrically clamped at both outer ends, beyond the wire wound regions, to a temperature reservoir held at ambient temperature. So the modern sensor designs differ from the Blackett design in that only finite length sections of the tube are uniformly heated, with unheated sections of tube in between, and beyond the heated portions. The modern sensors have abrupt steps or discontinuities in tube heater density that are not present in the Blackett sensor design or modeled in his equation. See Figure 2 below.

To accurately describe the heat flows and temperatures in modern sensor tubes requires solving a pair of coupled second order differential equations for the tube and fluid temperatures. The work of Hinkle and Mariano [4] showed in 1991 that the tube and gas axial temperature profiles are substantially different at flows within the normal range of modern sensors, so that the Blackett one equation modeling approach is not valid for modern sensors heated by multiple heater windings of finite length.

Before presenting the set of coupled differential equations valid for modern sensors it is appropriate to first describe more carefully the basic operating principle of these sensor tubes. That will be followed by a look at several simple exact particular solutions to these equations, which shed considerable light on the sensor physics and on the validity of the Blackett hypothesis for idealized sensors. Finally, some numerical solutions to the full coupled equations are given for typical modern sensors and more advanced designs based on spatially variable heater densities. These are compared and contrasted.

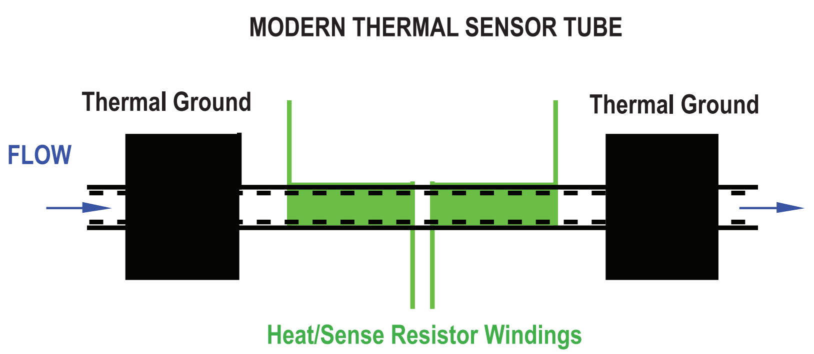

Figure 2. Schematic construction of modern laminar thermal sensor tube. Dimensions not to scale.

Operating Principle of the Tube Thermal Flow Sensor

Because this flow sensing technology is relatively new to the flow community a more thorough and careful explanation of the operating principle of the sensor is provided here for those who desire it. This section also provides a heuristic derivation of the fluid convection term in the heat conduction equations that are presented and solved later. (Those who are experts in heat conduction and differential equations may skip directly to Equations (3) ahead if they already understand the sensor.)

Capillary tube thermal mass flow sensors exploit the heat capacity of the fluid, which causes a fluid forced to flow through a conduit up a temperature gradient to absorb heat from the conduit wall, and a fluid forced to flow down a temperature gradient to give up heat to the conduit wall.

When a symmetrical temperature hill(in the direction of flow) is established by external heating means along an appropriate length of flow conduit, the fluid will transport heat absorbed from the upstream (uphill) portion of the conduit wall and deposit it to the downstream (downhill) portion of the conduit wall. When the heating power that generates the symmetrical temperature hill along the conduit wall is maintained constant independent of flow, the effect of the flow is to slightly reduce the temperature of the upstream conduit wall, and to slightly increase the temperature of the downstream conduit wall, by equal amounts. The difference between the downstream and upstream flow-induced conduit temperature shifts may be shown to be directly proportional to the product of fluid mass flow rate and fluid specific heat capacity, over a substantial flow range that depends on the fluid species.

To understand the basic operation of the sensing mechanism quantitatively, it is easiest to first consider an idealized situation, where the flow tube is assumed to have a precisely linear temperature profile maintained along its length. This situation is shown in Figure 3, to which reference should be made in the following discussion.

If the fluid inside the tube is not flowing, the fluid temperature will soon reach a thermal equilibrium where its temperature is everywhere equal to the temperature of the adjacent tube wall, so the fluid and tube will both have the same constant temperature gradient along the tube length. Now imagine the interior fluid to slowly flow through the tube at a constant rate, in the direction of increasing tube temperature, and consider what its equilibrium temperature must be, as a function of position along the tube. As each portion of flowing fluid passes from cooler to warmer positions along the tube, it will be heated by thermal conduction from the warmer tube wall. But it takes heat energy to raise the temperature of the fluid, because the fluid has a heat capacity.

The amount of energy required to heat the fluid mass m from temperature T1 to a slightly higher temperature T2 depends on the fluid specific heat capacity C_p, the fluid mass m, and the amount of temperature rise (T2-T1). If we denote the energy stored in the fluid heat capacity when the fluid temperature is raised from T1 to T2 by E, then we have the quantitative relationship $E = mC_p(T2-T1)$. Recalling that the temperature profile along the tube is a linear function of distance along the tube, we see that the heat energy required to move a given mass of fluid along the tube will be directly proportional to the length of tube traversed, so long as the axial temperature gradient along the tube is maintained constant.

If x denotes axial position along the tube, the energy per unit tube length needed to move mass m of fluid along a length of tube X2-X1 and raise its temperature from T1 to T2 will be

$$E/(X2-X1) = mC_p[(T2-T1)/(X2-X1)]. \quad (1)$$

Because the temperature gradient along the tube is constant in this ideal case, the right side of this equation will be the same for any two points 1 and 2 under discussion. So the heat energy per unit length absorbed by the fluid heat capacity as the mass of fluid travels along a tube with a linear temperature gradient is a constant independent of position along the tube, is directly proportional to the tube temperature gradient, and is equal to $mC_p dT/dx$, where we have replaced [(T2-T1)/(X2-X1)] with the constant axial temperature gradient dT/dx.

Taking time into consideration, we realize that for a constant flow of fluid the amount of mass m that will pass from X1 to X2 in a given time will be directly proportional to the fluid mass flow rate q_m and to the elapsed time, and we see also that a constant fluid

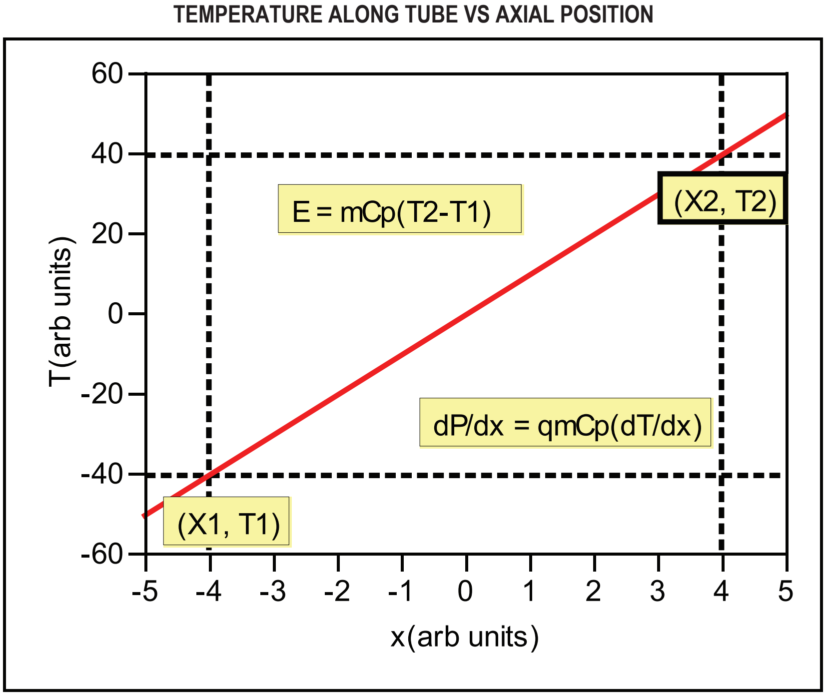

Figure 3. Idealized case: fluid flowing inside a tube with a linear temperature gradient along its length.

heating power per unit length of tube equal to

$$dP/dx = q_m C_p dT/dx. \quad (2)$$

is required in order to flow fluid at mass flow rate q_m through a uniform cross section tube with a constant positive temperature gradient maintained along its length. This expression is also locally valid (in the limit $dx \rightarrow 0$, $dP \rightarrow 0$) for heating power per unit length required to move fluid up a differential length of tube dx at location x when the tube temperature gradient varies with x.

How is this constant heating power per unit length provided to the fluid, since we have assumed only that the fluid is moving through the tube at a constant flow rate, and have not assumed any specific external mechanism to provide direct heating of the fluid?

Of course this heat must come into the fluid by radial thermal conduction from the adjacent tube wall that is in direct thermal contact with the flowing fluid. This can only happen if the tube at location x is warmer than the fluid at the same position, so that there may be a temperature difference to drive the radial heat conduction from the tube into the fluid. Since the required heating power per unit length is independent of lengthwise position (for a constant temperature gradient along the tube), and since the rate of radial heat transfer is directly proportional to the local temperature difference between tube wall and fluid, the temperature difference between tube and flowing fluid at location x must also be independent of lengthwise position x for a specified mass flow rate, fluid specific heat capacity and maintained tube temperature gradient. So we see that with steady flow the tube and fluid will reach a thermal equilibrium where both have the same lengthwise temperature gradient, but there will be a finite constant temperature offset between them independent of position x along the tube, and a corresponding radial conductive heat transfer per unit length between tube and fluid that is equal to the product of the mass flow rate, the fluid specific heat capacity, and the tube axial temperature gradient, as shown in Equation (2), provided only that the tube lengthwise temperature gradient is maintained constant.

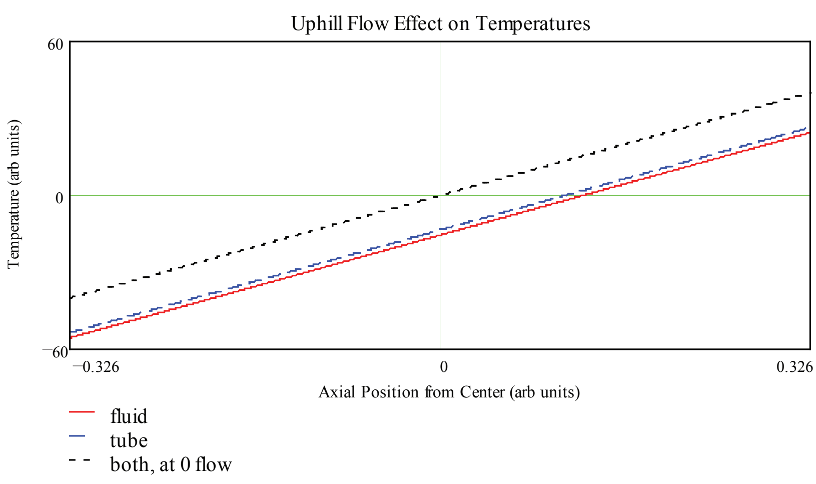

Figure 4. Flow through an idealized tube that has a positive constant temperature gradient maintained along its length, and its effect on fluid and tube temperatures. Flow is to the right in this plot, in the direction of increasing tube temperature. Dotted line shows both temperatures at zero flow, relative to the zero flow temperature at x=0, as a function of axial position x; solid line shows fluid temperature when flow is present; and dashed line shows tube temperature at the same flow.

Because heat is everywhere being radially conducted from the tube to the flowing fluid, it is evident that the tube temperature must be reduced by the flow, when the fluid is flowing up a temperature hill, compared to the zero flow tube temperature at each location (assuming the external heating power applied to the tube to maintain its constant temperature gradient is independent of flow). Both tube and fluid temperatures are reduced at all locations by the flow up the temperature hill, but the fluid temperature is reduced more than the tube temperature.

This situation is illustrated for a specific mass flow rate by Figure 4. For higher or lower flow rates both tube and fluid temperature offsets from the zero flow values will increase or decrease in direct proportion to the fluid mass flow rate.

When the tube temperature gradient is reversed, so that the fluid flows down the tube temperature gradient rather than up, it follows from the same logic that the fluid will reach a different equilibrium temperature that is equally higher than the tube temperature, as it was lower when the flow was up the temperature slope, so that radial thermal conduction from fluid to tube will remove the heat released from the heat capacity of the fluid as it flows down the tube temperature gradient (see Figure 5).

It will be evident to the thoughtful reader that any temperature distribution maintained along a tube that has upstream/downstream mirror symmetry about the sensor mid-length point at zero flow will function as a differential thermal flow sensor, with the upstream half of the sensor cooled by the flow and the downstream half warmed by the flow to the same extent. This must be because we can always imagine the symmetrical temperature profile as composed of many inlet differential lengths each of constant slope, each such differential length matched to one of opposite sign but equal magnitude slope on the outlet side of the sensor. We can imagine that each such differential length pair will function as an elementary flow sensor with a temperature offset directly proportional to the mass flow and to the local temperature gradient magnitude. The cumulative thermal effect of flow on all these elementary paired differential sensors in series will be to cool the inlet half of the sensor and warm the outlet half by the same amount, in direct proportion to the mass flow rate.

The question then arises which of the class of all symmetrical temperature distributions that might be employed for making such a sensor will perform best? And how can such an optimum tube temperature distribution be achieved in practice?

The temperature distributions employed in all existing mass production thermal flow sensor tubes are the ones that arise naturally from employing simple uniform resistive heater windings along the tube surface. Such windings produce heating density profiles along the tube length that are rectangular. These are convenient for sensor tube manufacture, but not necessarily optimum for sensor performance.

Differential Equations Governing the Sensor Action

It is a straightforward matter to derive the pair of linear coupled differential equations for the average steady state tube and fluid temperatures as a function of mass flow and position along the sensor tube. Here the equations will be stated, but, for brevity, not derived. They are essentially Fourier's equations for the temperature distribution along a uniform bar of constant cross-section, surrounded by a reservoir of air at constant temperature, with Newton's Law of Cooling applied at the bar outer surface, and with the bar heated by an external source that is an arbitrary function of axial position. Here the bar is a hollow tube that has a cylindrical column of fluid flowing inside, so that a second Fourier equation is needed to determine the temperature distribution along the interior 'bar' of fluid. The solid and fluid bars are laterally coupled thermally at their common interface surface, again by a Newton's Law of Cooling condition. A new term is added to the fluid thermal heat conduction equation to account for energy exchanges with the fluid heat capacity as the flowing fluid changes temperature. This is just the expression previously derived in Equation (2) for the special case of a constant axial temperature gradient maintained along the tube. Finally. a heat source term is formally added to the fluid equation to account for fluid heating by viscous friction in the fluid, though this heat source is known to be negligible for the flow rates under conditions normally used in modern gas flow thermal sensors. See Equations (3) below.

Note that all terms in both equations have dimensions of watts/meter, where

x = the coordinate that specifies axial position along the sensor tube length;
T(x) = the tube temperature averaged over the transverse tube cross-section at position x (°C);
$T_F(x)$ = the fluid temperature averaged over the transverse fluid cross-section at position x(°C);
T_0 = the temperature of the ambient surround outside the tube, assumed independent of x;
q_m = fluid mass flow (constant, independent of x);
λ(x) = the local heating power density externally applied to the tube at x (in watts/meter);
H' = a constant specifying tube outer surface heat loss, w/units watts/(meter · °C);
H = a constant specifying tube inner surface heat loss, w/units watts/(meter · °C);
T_v = the elevation of fluid temperature due to fluid viscous heating;
A, A_F = the cross-sectional areas of the tube and fluid, respectively, independent of x;
K, K_F = the tube and fluid thermal conductivities, respectively, in units of watts/(meter · °C); and
C_{Fp} = the fluid specific heat capacity at constant pressure, in joules/(kg · °C).

$$
\begin{aligned}
&-K \cdot A \cdot \frac{d^2T(x)}{dx^2} + H' \cdot (T(x) - T_0) + H \cdot (T(x) - T_F(x)) = \lambda(x) \\
&-K_F \cdot A_F \cdot \frac{d^2T_F(x)}{dx^2} + q_m \cdot C_{Fp} \cdot \frac{dT_F(x)}{dx} + H \cdot (T_F(x) - T(x)) = H \cdot T_v
\end{aligned} \tag{3}
$$

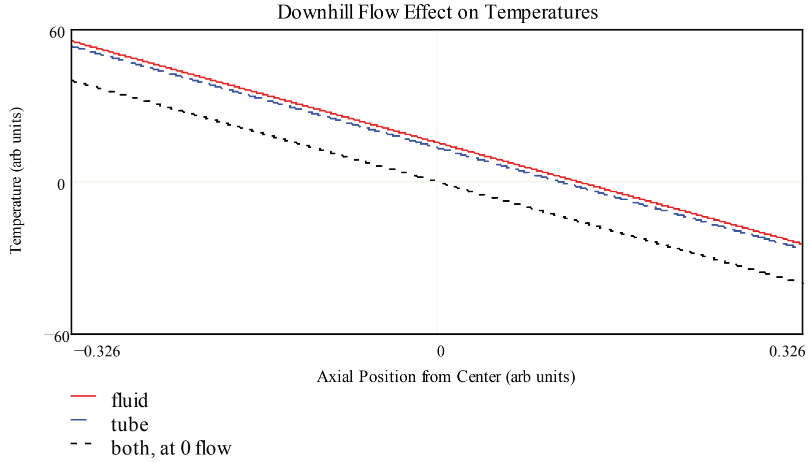

Figure 5. Flow through an idealized tube that has a negative constant temperature gradient maintained along its length, and its effect on fluid and tube temperatures. Flow is to the right in this plot, in the direction of decreasing tube temperature. Dotted line shows both temperatures at zero flow, relative to the zero flow temperature at x=0, as a function of axial position x; solid line shows fluid temperature when flow is present; and dashed line shows tube temperature at the same flow.

Of course the arbitrary heater density function λ(x) must be specified by giving the location and dimensions of the heat/sense resistive windings and the electrical power converted to heat in them, before the fluid and wall temperatures can be calculated from Equations (3), Likewise, the tubing dimensional parameters and thermal properties, and the fluid thermal and material properties, plus the mass flow rate, plus the surface heat transfer parameters, must be specified before the equations can be solved for specific sensors.

Because the length of these sensor tubes is typically hundreds of times longer than the diameter, it is the axial temperature dependence of the tube and fluid temperatures that most strongly influences the sensing action, temperature differences within each medium in the radial direction are either very small (through the tube wall thickness), or well known (for a simple laminar flow profile in a fluid of known viscosity), so that a radially-lumped, axially continuous theoretical model should be able to account satisfactorily for the major features of sensor behavior without getting bogged down in the intricacies of coupled partial differential equations in three spatial dimensions in a cylindrical geometry. At the same time the inadequacies of the single-equation Blackett theory pointed out by Hinkle and Mariano are avoided by allowing the tube and fluid to have dramatically different average temperatures at the same axial location, to the extent consistent with the known physical laws of heat conduction.

Equations (3) work well for the design and analysis of modern thermal sensors, and no simpler theoretical model accounts for all the effects observed. They are tricky to solve for modern sensor geometries, leading some to make injudicious simplifying approximations that lead to false results. For those who persevere and succeed in solving them however, the rewards in understanding of the sensor behavior are substantial.

Are There Any Simple Closed Form Solutions?

In the tradition of E. Fermi we look first to see if there are any especially simple situations where exact closed-form solutions to the coupled equations exist, that will help us understand the basic physics of the device.

Of course there is the trivial case of an infinitely long tube where the external heating power delivered through the windings is everywhere zero, so that the tube and fluid temperatures must be independent of x for all x. We would not expect to get any sensing action in this case.

Constant Heater Density for All x

However, this trivial case is included in the slightly less trivial case of an infinitely long tube with a heating density that is constant, independent of x. This is produced by extending the uniform resistive heater winding to cover the full (infinite) tube length. In this case we expect to find a solution where the fluid and tube temperatures are independent of x, so that their derivatives are 0 and Equations (3) reduce to a pair of linear algebraic equations for T_F and T. The solutions are

$$T(x) = T_0 + \frac{\lambda_0}{H'} + \frac{H}{H'} \cdot T_v \quad \text{and} \tag{4}$$

$$T_F(x) = T_0 + \frac{\lambda_0}{H'} + \left(\frac{H}{H'} + 1\right) \cdot T_v \, .$$

These are independent of x but also independent of mass flow rate q_m, (except for the negligibly small term in T_v). These also show that the very weak frictional heating due to fluid viscosity causes an elevation of the fluid temperature above the tube temperature by the amount T_v. So heating the tube uniformly produces no flow sensing action in itself, and an infinitely long sensor tube with a uniform heater winding would produce no flow signal.

Why then does Blackett's sensor design work, since it has a uniform heater density along the whole tube length? Because his sensor has finite length, and the ends of the tube are thermally clamped at ambient temperature, but the entire tube length is heated above ambient, so that the gas undergoes a substantial temperature rise in flowing from the cool inlet end to the hot center of this uniformly heated sensor tube. A temperature hill of some sort must be produced along the tube, before any mass flow sensing effect can occur. Symmetrical temperature hills work best, because they are readily configured as differential flow sensors.

The usual technique for solving Equations (3), once given the specific input information about the fluid and tube materials and the geometrical dimensions of the sensor tube, is to eliminate one or the other of the two unknown temperature distributions by algebraic manipulation, so that a single fourth-order differential equation in only one of the axial temperature profiles results. Because this is a linear differential equation with constant coefficients, one can find the general solution by adding the solution of the homogeneous equation (a sum of 4 exponentials in x, valid when no heat sources are present) to a particular solution valid for the specific non-zero heater density actually applied. Four thermal boundary conditions must then be applied to determine the four unknown constants of the four exponentials. The natural boundary conditions to impose are to specify the tube and fluid temperatures at both ends of the sensor, where the tube is physically clamped to a thermal ground.

For conventional uniform winding sensors, the particular solution is given by Equation (4), for x within a heated region (tube portion covered by a heating winding), and by Equation (4) with λ_0=0 for x outside a heated region. So there is a discontinuous step in the particular temperature solution at each end of each winding. A temperature discontinuity cannot normally exist in nature, and it does not either in the mathematics that correctly describes nature. The four exponentials of the homogeneous solution smooth out the discontinuity of the particular solution at the ends of the heaters, and yield a fluid temperature distribution that is smooth and continuous through the first 3 spatial derivatives, despite the finite discontinuity of the heater density at the winding ends. However, for this uniform heater sensor geometry the entire flow dependence occurs in the exponentials of the homogeneous solution, while the particular solution for the tube temperature has no flow dependence at all. The flow dependence is locked up in the exponential constants, where it is implicit and relatively inaccessible for purposes of understanding the sensor action. (For example, for this geometry Blackett's Hypothesis can best be tested numerically.)

The search for simple solutions that yield understanding of these sensors has hit a dead end in the analysis of the conventional sensor geometry, with its excessively complicated mathematics.

Constant Axial Temperature Gradient for All x

Yet the idealized case of the constant axial temperature gradient maintained along the tube provided significant insight into the sensing action. We can look for a particular temperature profile that is linear in x by substituting linear functions for both $T_F(x)$ and T(x) into the governing Equations (3), and using the equations themselves to determine the 4 unspecified coefficients needed for the two linear temperature functions. All the second derivatives then drop out of the equations, and we get a simple result.

$$T(x) = T_0 + \frac{H}{H'} \cdot T_v - \frac{q_m \cdot C_{Fp}}{H'} \cdot B + B \cdot x \qquad (5)$$

$$T_F(x) = T_0 + \left(\frac{H}{H'} + 1\right) \cdot T_v - q_m \cdot C_{Fp} \cdot B \cdot \left(\frac{1}{H} + \frac{1}{H'}\right) + B \cdot x$$

B here is the axial temperature gradient maintained along the tube. In order to get this simple exact solution we must accept the condition

$$\lambda(x) = H' \cdot B \cdot x \,. \qquad (6)$$

The heater density function must be a linear function of x in order for tube and fluid temperatures to be linear functions of x. This exact particular solution is mathematically valid over the infinite x range, and no complicating exponentials appear. In addition, the particular solution itself has an explicit flow dependence that we can test for agreement with Blackett's hypothesis.

Let's do that. Examining the term proportional to the mass flow q_m in T(x) we find a flow induced temperature offset of $-(q_m \cdot C_{Fp}/H') \cdot B$, so the tube temperature is depressed in proportion to the mass flow rate multiplied by the fluid specific heat. The other factors appearing, H' and B, are the tube outer surface loss coefficient per unit length, and the imposed constant temperature gradient B, that are both independent of the properties of the interior gas. So Blackett's Hypothesis is confirmed exactly for the flow-induced tube temperature offset in this particular case.

This is not the case for the flow-induced *gas* temperature offset. Examining the flow dependent term in $T_F(x)$ we see that it depends on H, the tube interior surface loss coefficient, which depends on the thermal conductivity of the flowing fluid. The laminar tube flow sensor obeys Blackett's hypothesis because it measures the *tube* temperature offset, not the *gas* temperature offset.

We can imagine a differential thermal flow sensor based on a temperature hill that has the shape of a symmetrical triangle, sloping up, and then down. At points far from the peak the equations above will describe the temperature profiles on the upstream and downstream halves (with B's of opposite sign), so we can easily compute the upstream —downstream temperature difference caused by the flow. This is

$$Tdn - Tup = 2 \cdot \frac{q_m \cdot C_{Fp}}{H'} \cdot B \,. \qquad (7)$$

Note that this particular exact solution to the general coupled differential equations not only tells us that a linear temperature profile along the tube is possible, it also informs us that this can be achieved by making the applied heater density a specific function of position along the tube. This can be achieved in practice by varying the pitch of the heating winding with position along the tube. The axially variable heater density approach to thermal flow sensor design has been patented [5].

Symmetrical Heater Density Quadratic in x

A more stringent theoretical test of Blackett's Hypothesis requires a more realistic temperature hill with a natural maximum, but not a constant gradient. Trying an inverted symmetrical parabola for the spatially variable heater density

$$\lambda(x) = \lambda_0 - \lambda_2 \cdot x^2, \text{ with } \lambda_0, \lambda_2 > 0 \qquad (8)$$

we find the quadratic temperature profiles in the Equation (9) below:

$$T(x) = T_0 + \frac{\lambda_0}{H'} + \frac{H}{H'} \cdot T_v - \frac{\lambda_2}{H'} \cdot \left[\left(x - \frac{q_m \cdot C_{Fp}}{H'}\right)^2 + \left(\frac{q_m \cdot C_{Fp}}{H'}\right)^2 + \frac{2 \cdot (q_m \cdot C_{Fp})^2}{H' \cdot H} + \frac{2 \cdot (K \cdot A + K_F \cdot A_F)}{H'}\right] \qquad (9)$$

$$T_F(x) = T_0 + \frac{\lambda_0}{H'} + \left(1 + \frac{H}{H'}\right) \cdot T_v - \frac{\lambda_2}{H'} \cdot \left[\left[x - q_m \cdot C_{Fp} \cdot \left(\frac{1}{H'} + \frac{1}{H}\right)\right]^2 + \left[q_m \cdot C_{Fp} \cdot \left(\frac{1}{H'} + \frac{1}{H}\right)\right]^2 + 2 \cdot \left[\frac{K \cdot A}{H'} + K_F \cdot A_F \cdot \left(\frac{1}{H'} + \frac{1}{H}\right)\right]\right].$$

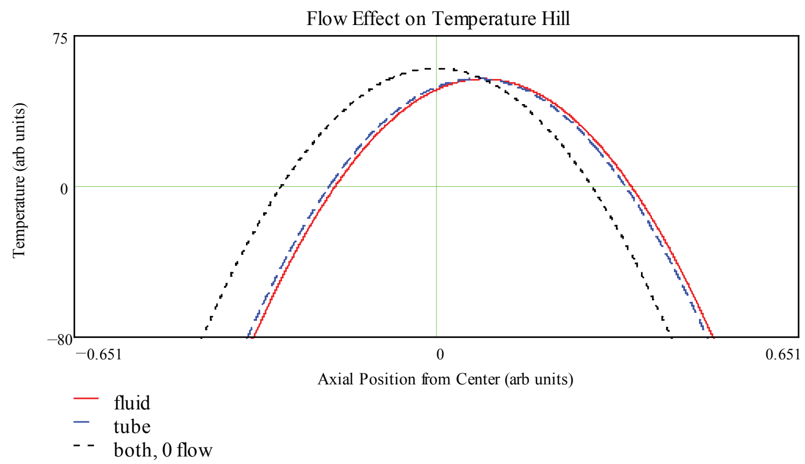

Figure 6. Idealized tube that has a symmetrical parabolic temperature hill along its length at zero flow, and the effect of flow on fluid and tube temperatures. Flow is to the right in this plot. Dotted line shows both temperatures at zero flow, relative to an arbitrary value at x=0, as a function of axial position x along the sensor tube. Solid line shows fluid temperature when flow is present; and dashed line shows tube temperature at the same flow.

A plot of these exact solutions, (with and without flow) is shown in Figure 6.

The flow-induced temperature offsets are now a function of x as well as mass flow. Figure 7 shows the Tube-Fluid temperature difference as a function of x, at a specific flow. This difference drives the radial conduction between tube and fluid.

Since the tube axial temperature profile is now exactly known as a function of x for this idealized model system, we can calculate the difference in average temperature between the downstream and upstream halves of a length L of the sensor tube centered at the midpoint, x=0, and determine the dependence on mass flow. We write

$$Tdn - Tup = \frac{2}{L} \cdot \int_{0}^{\frac{L}{2}} T(x)dx - \frac{2}{L} \cdot \int_{-\frac{L}{2}}^{0} T(x)dx . \qquad (10)$$

Making a change of variable from x to –x in the second integral gives

$$Tdn - Tup = \frac{2}{L} \cdot \left[\int_{0}^{\frac{L}{2}} T(x)dx - \int_{0}^{\frac{L}{2}} T(-x)dx \right] . \qquad (11)$$

Any part of the tube temperature profile with even symmetry in the presence of flow will make no contribution to the difference Equation (11), so we need only integrate the odd part of the tube temperature profile, which is a single term proportional to x.

$$T_{odd}(x) = 2 \cdot \frac{\lambda_2}{H'} \cdot \left(\frac{q_m \cdot C_{Fp}}{H'} \right) \cdot x \qquad (12)$$

$$T_{odd}(-x) = -T_{odd}(x)$$

The downstream – upstream average temperature difference over the finite symmetrical central length L of the sensor tube in the presence of flow is now

$$Tdn - Tup = \frac{4}{L} \cdot \left[\int_{0}^{\frac{L}{2}} T_{odd}(x)dx \right] = \frac{4}{L} \cdot 2 \cdot \frac{\lambda_2}{H'} \cdot \left(\frac{q_m \cdot C_{Fp}}{H'} \right) \cdot \left[\int_{0}^{\frac{L}{2}} xdx \right]$$

$$Tdn - Tup = \frac{\lambda_2}{H'} \cdot \left(\frac{q_m \cdot C_{Fp}}{H'} \right) \cdot L . \qquad (13)$$

Clearly, in this case also the flow-induced downstream – upstream average tube temperature difference is directly proportional to the product of mass flow rate q_m and fluid specific heat capacity C_{Fp}, and dependent on no other property of the fluid flowing in the tube, just as Blackett proposed in 1930. While this does not prove Blackett's Law for the general case, it certainly shows that a constant temperature gradient along the tube is not necessary to make a thermal sensor that satisfies Blackett's Hypothesis. This makes it more plausible that commercial sensors with uniform finite windings also satisfy Blackett.

Heater Density Any Finite Polynomial in x^2

A heater density that has the functional form of a finite degree polynomial in x^2 will always produce a symmetrical temperature hill at zero flow, and will apparently also generate a closed form particular polynomial solution of Equations (3) valid at arbitrary laminar flows for that specific heater density. One can generate the particular solution by substituting general polynomials for T(x) and $T_F(x)$ in x of the same maximum degree as the heater density for both fluid and tube temperatures into the differential equations, and equating the coefficients of individual powers of x. Taking the coefficients of the heater density polynomial as

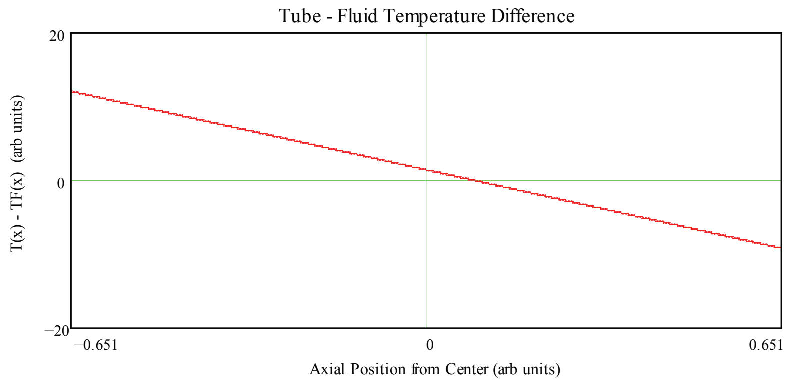

Figure 7. Idealized tube that has a symmetrical parabolic temperature hill imposed along its length Effect of flow on tube - fluid temperature difference. Flow is to the right in this plot. Red line shows tube – fluid temperature difference vs. x corresponding to Fig.6. In the absence of flow the temperature difference would be nearly 0, independent of x. A higher flow would increase the magnitude of the slope of the red line and displace it further to the right.

known, all the coefficients of the fluid and tube temperature polynomials may be found as functions of the given heater density coefficients and the system parameters and constants appearing in the differential equations.

As one increases the maximum degree of the heater density function, this algebraic process becomes increasingly tedious, and the functional forms of the polynomial coefficients become increasingly complicated functions of the system parameters and the flow. However, these are exact polynomial solutions of the system equations for the tube and fluid temperature profiles, on the infinite x domain, with the flow dependence of the sensor system given as explicit algebraic functions of the system design parameters. The tube temperature profile function can be integrated over each half of the heater length, giving an exact analytical function for the flow dependence of the sensor output signal (downstream–upstream mean tube temperature duifference) as a known function of the system design parameters and the mass flow rate.

The author has also worked out the solutions for the general 4th degree heater density polynomial, but they are not given here because of their greater complexity.

Such exact solutions to the sensor system differential equations are useful for several purposes:

- They can be studied to better understand the action of this class of flow sensors.
- They can provide benchmarks for testing more elaborate sensor models (finite elements).
- Sensors can be designed to mimic them in order to take advantage of the known exact solutions.
- They can be used (as here) to test suggested empirical correlations such as Blackett's Hypothesis.
- They suggest ways to tailor the tube axial temperature profile to improve sensor performance.

What Do the Particular Solutions Tell Us About Sensors?

The exact solutions for the linearly ramped and parabolic heater densities on the infinite domain show a precisely linear response to flow that has no upper limit. This is in striking contrast to existing real sensors, where the sensor output always reaches a maximum and then gradually falls to zero as the flow is further increased (while remaining in the laminar range). Yet the same theoretical equations also correctly predict the onset of flow sensor non-linearity when used to model conventional sensors with rectangular heater density distributions. If the sensor non-linearity effects are contained in the basic equations, why do they not appear in the case of these particular simple solutions to idealized cases? Is this related to their infinite length? Is the nonlinear flow response with the rectangular heater profiles caused by the need to include the characteristic exponential solutions to satisfy the end boundary conditions? If so, attempting to use one of the particular solutions for a finite length sensor would also require the characteristic exponentials to meet end boundary conditions, so introducing undesired sensor non-linearity. (But perhaps not so much as in the case of the uniform heater density, where the entire flow signal comes from the characteristic exponentials.)

Because uniform heating along an infinitely long tube produces no flow signal, all conventional sensors heated by uniform windings are end-effect sensors, deriving their flow sensitivity from the abrupt steps in heater density that occur at the ends of the windings. The optimum length for such sensor windings is determined by the distance that the end thermal transients penetrate into the interior of a long winding. The windings should be just long enough to make the heated tube temperature approach the theoretical maximum, but not so long that the tube temperature profile exhibits an extended interior plateau. In this way the two uniform winding symmetrical sensor becomes "all end" and most effective for flow sensing. If it is properly designed making it either longer or shorter would only degrade its performance.

In contrast to the conventional uniform rectangular heater density, the linearly rising heater density is equally sensitive to flow at every point along its length, so can be made arbitrarily long on a particular tube without losing flow sensitivity. The parabolic hill heater density, with the axial gradient increasing as one moves away from the peak, can also be made arbitrarily long, with the flow sensitivity increasing in proportion to the length. Neither one of these variable heating density configurations is limited to a fixed length on a given tube, as the conventional design is. But there is a limit to how short they can be made on a given tube. They are 'minimum length' sensors rather than 'fixed length' sensors.

But what advantages might be expected from longer sensor tubes? Increased linear flow range of the sensor, for one, and also better flow resolution. Their use should also greatly reduce the confusion regarding the 'gas correction factors.'

The primary reason, in the author's view, for the disagreement among manufacturers about the empirical conversion factors used for scaling thermal sensor response from one gas to another, is that most manufacturers deliberately chose their sensor full scale (for N_2) to be at a flow where the sensor tube is already slightly non-linear, i.e. outside the flow range where Blackett's Hypothesis is expected to be valid. Then different manufacturers are willing to tolerate different amounts of N_2 non-linearity at sensor full scale. This in itself is sufficient to ensure different gas correction factors measured empirically relative to N_2.

N_2 is not the most non-linear gas in thermal sensors, so there will be

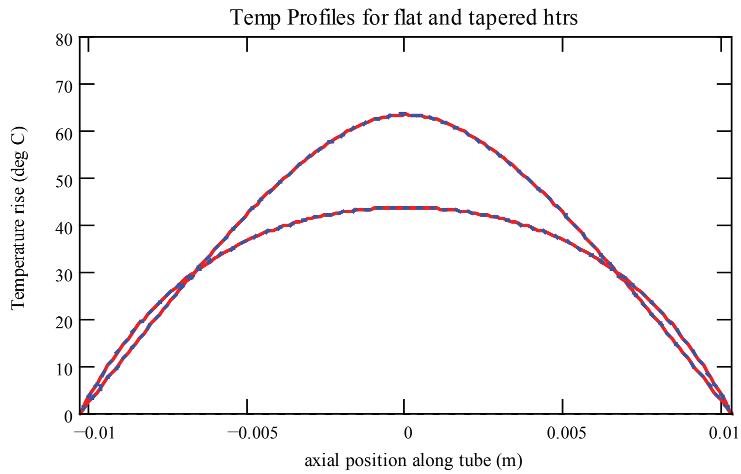

Figure 8. Temperature profiles produced along the same tube by uniform heater density and symmetrical triangular heater density with the same total power, at 0 flow.

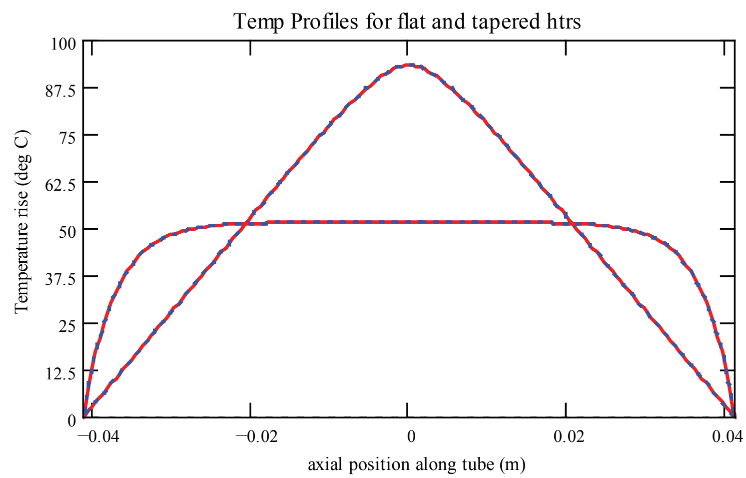

Figure 9. Making sensor 4X longer shows the flat sensor is end-effect but tapered sensor sensitive full length.

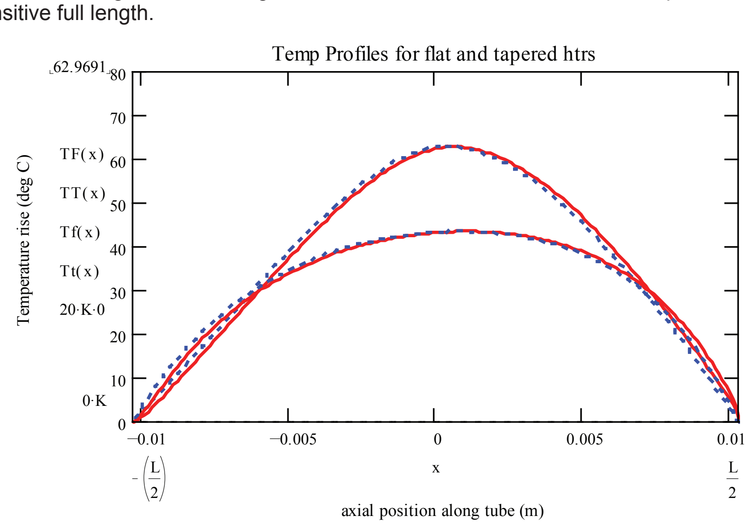

Figure 10. Temperature profiles produced along the tube of Fig. 8 by uniform heater density and symmetrical triangular heater density with the same total power, at 5 sccm N2 flow. Solid is fluid, dashed is tube.

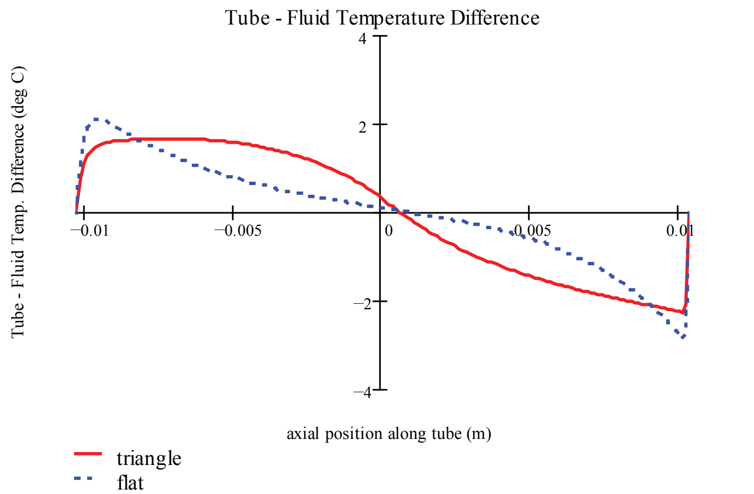

Figure 11. Tube – Fluid temperature differences at flow of 5 sccm N2, for the sensor heater configurations of Fig. 8.

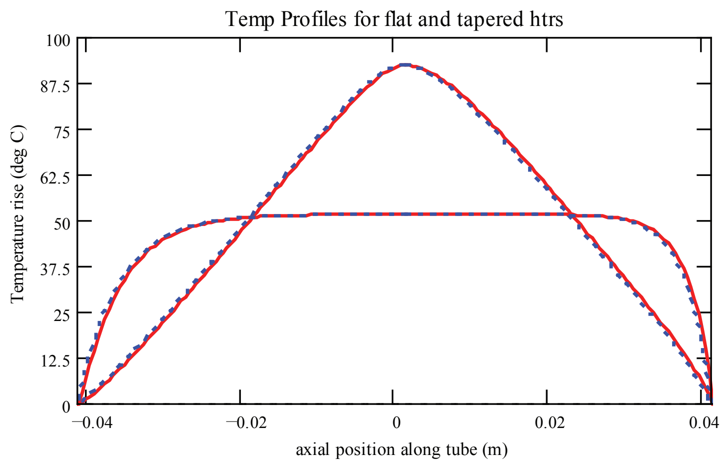

Figure 12. Temp. profiles produced along the 4X longer tube of Fig.9 by uniform heater density and triangular heater density with the same total power, at 5 sccm N2 flow. Solid is fluid, dashed is tube.

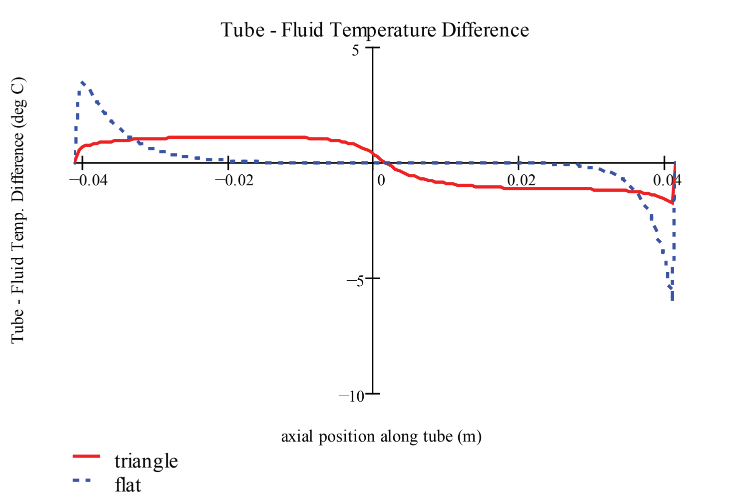

Figure 13. Tube – Fluid temperature differences at flow of 5 sccm N2, for the 4X longer sensor heater configurations of Fig. 9.

other gases where the sensor is even more non-linear at the corresponding full scale point, and this will make the gas correction factor appear to be variable with flow (i.e. a gas correction function). These gas discrepancies among manufacturers could potentially be greatly reduced by introduction of significantly more linear thermal sensors.

The ideal zero flow temperature profile for a sensor tube appears to be the symmetrical triangle, because (except at the apex) all second derivative terms in the heat conduction equations vanish. Fluid convection and radial conduction to the wall then dominate the fluid heat balance, and the flow sensing action is cleanest. Interfering axial thermal conduction effects are absent. This can be realized in a differential sensor by using a heater density function shaped like an Isosceles triangle.

Rectangular vs. Triangular Heater Densities

To solve the heat transfer equations for an Isosceles triangle heater density one can split the x domain into two parts, and use the particular solutions already found for the linearly rising and falling temperature profiles, with the division point at x=0. However, the resulting discontinuity in temperature slope at the apex is unphysical, and must be removed by adding characteristic exponential solutions to smooth out the temperature profiles at x=0. These round off the peaks in the temperature profiles, but introduce a tube-dependent length scale that limits how short the triangle profile sensor can be on a given tube. Figures 8 and 9 illustrate the two axial temperature profiles produced by rectangular and symmetrical triangular heater densities delivering the same power on the same tubing. Figure 9 is 4X longer, with 4X the heating power. The tapered heater density achieves higher peak temperature and a more constant temperature gradient on the

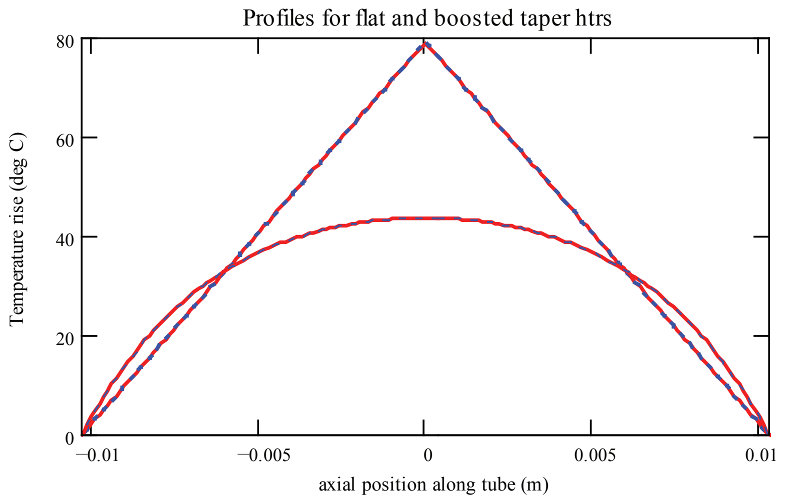

Figure 14. Temperature profiles produced along the same tube by uniform heater density and boosted symmetrical triangular heater density with the same total power, at 0 flow.

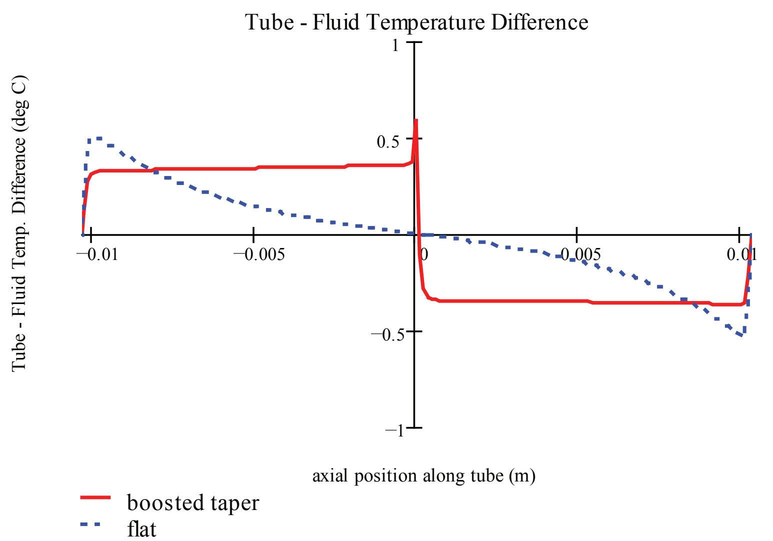

Figure 15. Tube – Fluid temperature differences at flow of 1 sccm N2, for the sensor heater configurations of Fig. 14 Note the contrast between difference profiles produced by the end-effect uniform heater density (dashed) and the boosted triangular heater profile (solid). Both have the same total power.

sides. The uniform heater density produces a smaller, flatter maximum and a steeper gradient near the ends. The steeper gradient at the ends means more heating power is lost into the end clamps.

Figure 10 shows the temperature profiles for both heater profile cases of Figure 8 for both fluid and tube, for a flow of 5 sccm. One can see that the tube temperature is higher than the fluid on the inlet end and lower than the fluid on the outlet end. To see the flow-induced tube-fluid temperature differences clearly requires an expanded plot of those differences vs. x, shown in Figure 11.

It is evident from Figure 11 that the triangular heater density produces a greater temperature difference at most positions along the tube than the uniform heater density, and those differences are more evenly distributed over the length. The flow effects are much more concentrated at the ends for the uniform heater density.

Examining the flow-induced temperature profiles at 5 sccm N2 in for sensors 4x longer in Figures 12 and 13, we observe that the triangular heater density sensor continues to be active over its full length, but the rectangular heater density sensor has activity only near its ends. Most of the length of its two winding coils is dead resistance that produces no flow signal. Increasing the length for the tapered heater sensor made its temperature profiles conform more closely to the triangular ideal. The tube – fluid temperature difference becomes nearly constant but of opposite sign for the inlet and outlet halves of the tube powered by the triangular heater density.

Rectangular vs. Boosted Triangular Heater Densities

The use of a symmetrical triangular heater density instead of the conventional rectangular heater density offers advantages by distributing the sensing action equally over the sensor length, and allowing the linear range of the sensor to be greatly increased by using longer sensor windings on any given tube. But there seems to be a limitation at short lengths due to the blunting of the sharp heater density apex in the tube and fluid temperature profiles.

Is there any way to produce a sharply pointed triangular temperature profile along the tube even at short sensor lengths? Yes. A concentrated point heater on a long tube will produce a tube temperature profile that has a slope discontinuity at the location of the point heater. By combining such a discrete point heater of appropriate strength with a continuous symmetrical triangular heater it is possible to generate a truly triangular tube temperature profile of any length. Such heater designs are called boosted tapered heaters. Figure 14 shows the temperature profiles predicted for such a heater density in comparison to a rectangular heater density of the same total power on the same tube. The sharpness of the triangle apex is evident.

The expected tube-fluid temperature difference in response to flow is shown in Figure 15 for a flow of 1 sccm N2. As expected from the sharpness of the triangle apex for both tube and fluid temperature profiles, the difference temperature is nearly ideal, nearly constant over the length with a very sharp transition to the opposite sign at the sensor midpoint. The rectangular heater density in contrast, again yields a tube – fluid temperature profile that is smaller and localized near the sensor outer ends.

The use of the booster point heater with a symmetrical triangular heater density completely solves the problem of producing a triangular zero flow temperature profile on any straight sensor tube with uniform properties along its length. It will work with sensors of any length on any tube, for any sensor system governed by Equations (3). However, the linear flow range of any such sensor will still be dependent on total sensor length. Making the sensor very short will reduce the linear flow range and also become increasingly wasteful of heating power, as the maximum profile temperature drops due to the large proportion of the heating power being conducted into the thermal clamps for very short sensors.

At high flows the temperature profiles of both tube and fluid will eventually be distorted by the thermal loading effects of the fluid convection, this being a source of nonlinearity in the sensor. Figures 16 and 17 show these effects for the boosted tapered heater and the normal rectangular heater at a flow of 10 sccm N2 for the nominal length sensor modeled. Note that the point booster heater pins the tube temperature maximum at x=0 so the thermal loading mainly curves the sides of the triangle. In contrast the peak of the uniform heater tube temperature is displaced downstream by a significant amount.

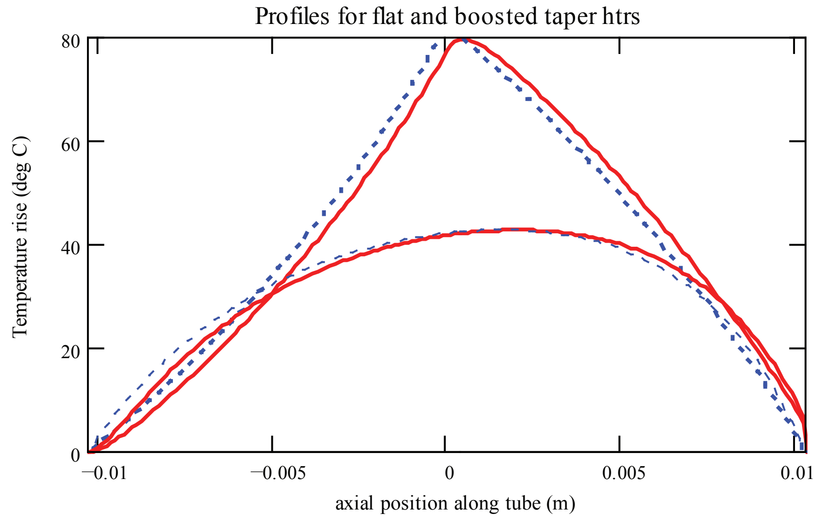

Figure 16. At 10 sccm N2 both boosted taper and rectangle heater fluid and tube profiles become distorted. Solid curves are fluid temperatures, dashed curves are tube temperatures. Compare Fig.14 at 0 flow.

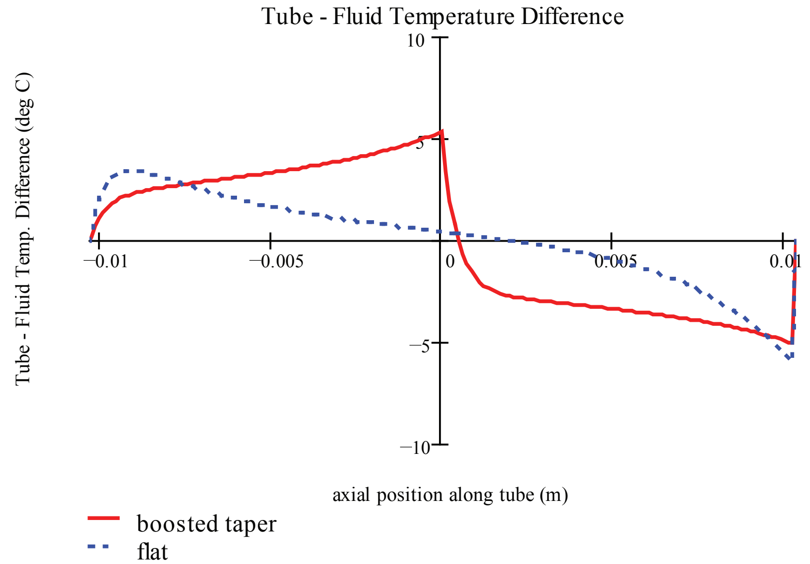

Figure 17. Difference Temperature Profiles at 10 sccm N2, where sensor responses are becoming non-linear. Compare to Fig.15 above, in the flow range where the sensor responses are much more linear.

Implementation of Boosted Tapered Concept

Point heaters have zero dimension so are mathematical abstractions. They also have physically unrealizable infinite heater density. To actually make a boosted tapered heater one must use a finite width heater with finite heater density as a booster, so one is led to examine designs for center heater regions of finite width that are placed between symmetrical inlet and outlet linearly tapered heaters, sometimes with small gaps between windings as is commonly the case in tapered heaters produced by varying the pitch of the heater windings along the sensor tube length. Figures 18, 19, and 20 illustrate how an acceptable triangular temperature profile along a sensor tube can be built up from the combination of a narrow central uniform booster heater and a pair of symmetrical linear tapered heaters disposed on both sides. First the central uniform booster heater alone and its temperature distribution are shown (Figure 18); then the pair of tapered heaters alone with their corresponding temperature distribution (Figure 19); and thirdly, the sum of booster and tapered heaters of the previous cases and its temperature distribution, which is essentially triangular, is shown. Note that the triangle apex is not perfectly sharp but is rounded on the scale of the central booster width.

Figure 21 shows the predicted tube—fluid temperature difference distribution for this heater geometry, along with the heater density itself, at a flow of 0.5 sccm N2. Outside of the width of the central booster heater, the desired constant offset proportional to flow with opposite sign on inlet and outlet is achieved.

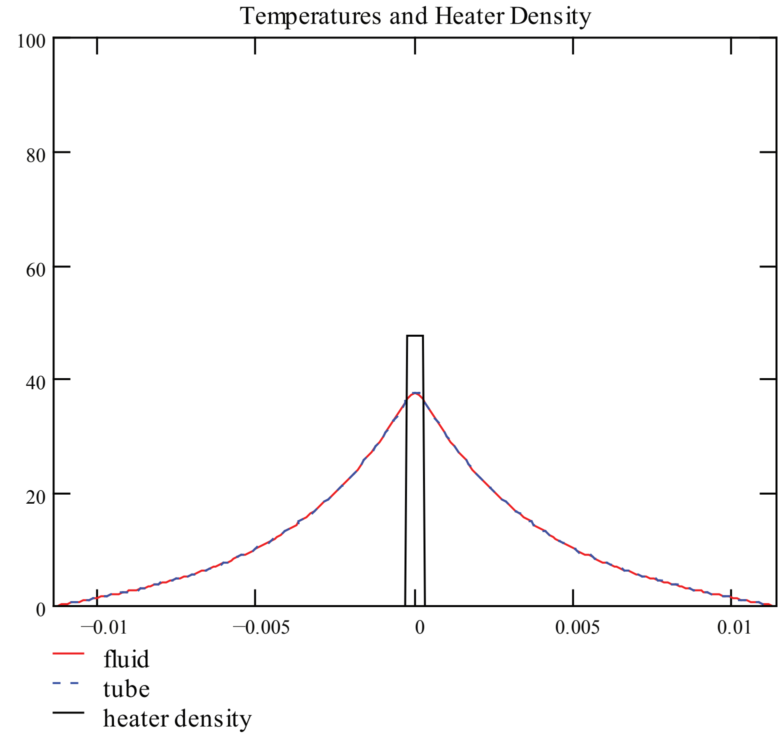

Figure 18. Center booster heater realization alone and its temperature profiles, 0 flow.

Conclusion

It should be understood by the reader that the thermal laminar sensor tube technology is not mature, because today's sensor tubes do not utilize an important design degree of freedom, the ability to make the heater density a function of position along the sensor length in order to control the shape of the temperature profile along the tube.

If we were at an equivalent stage in roof design as we are in thermal sensor design, all roofs would have flat tops; there would be no pitched roofs. If we were at an equivalent stage in boat design, there would only be flat-bottomed rectangular barges, no pointed bows or streamlined hulls.

The author invites suggestions as to how the non-uniform heater density sensing concept may best be brought into productive use for flow measurement and control.

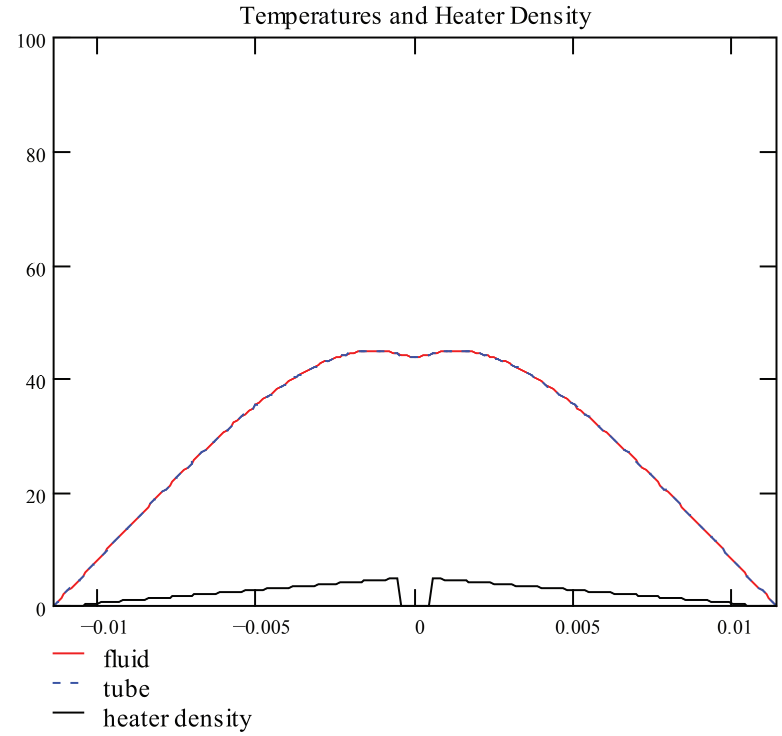

Figure 19. Linearly tapered heaters alone and their temperature profile, 0 flow.

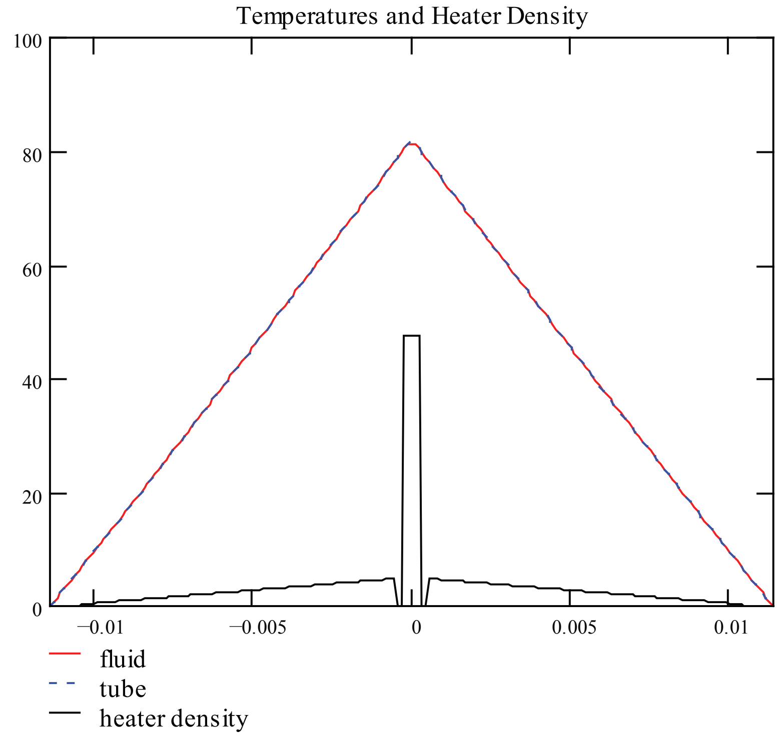

Figure 20.Combination of uniform central booster and linearly tapered heaters and the resulting triangular temperature distribution at 0 flow.

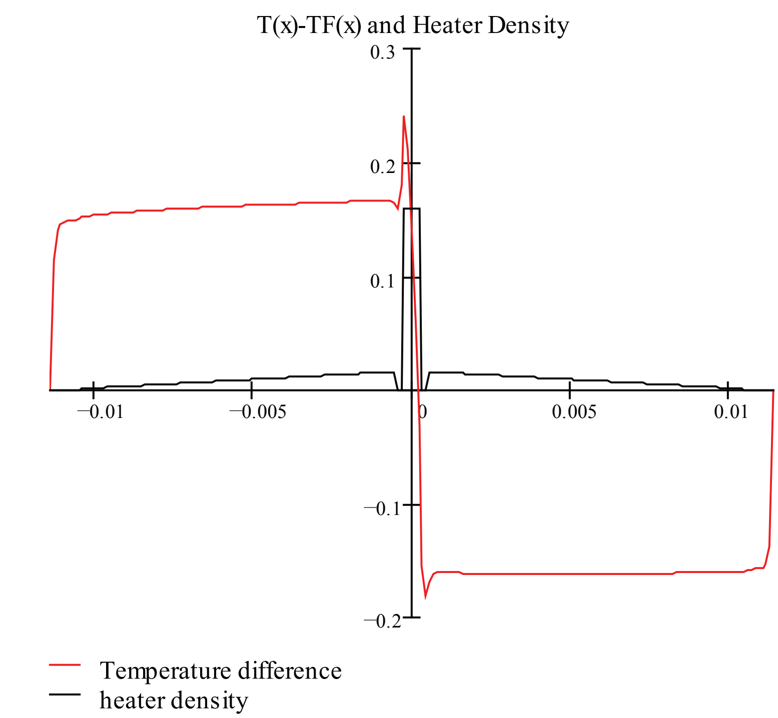

Figure 21. Tube – Fluid Temperature difference profile along the sensor for the heater configuration shown, at a flow of 0.5 sccm N2.

References

[1] P.M.S. Blackett, P.S.H. Henry, and E.K. Rideal , "A Flow Method for Comparing the Specific Heats of Gases," *Proc. R. Soc. London SeR.* A 126, (1930) 319-354.

[2] S.A. Tison, "A Critical Evaluation of Thermal Mass Flowmeters," *J. Vac. Sci. Technol.* A14 2582 (1996).

[3] K. Komiya, F. Higuchi, and K. Ohtani, "Characteristics of a Thermal Gas Flowmeter," *Rev. Sci. Instrum.* 59, 477 (1988).

[4] L.D. Hinkle and C.F. Mariano, "Toward Understanding the Fundamental Mechanisms and Properties of the Thermal Mass Flow Controller," *J. Vac. Sci. Technol.* A9, 2043 (1991).

[5] T. Maginnis, US Patent # 5,693,880 "Heater with Tapered Heater Density Function for Use with Mass Flowmeter"; US Patent # 6,446,504 B1 "Constant Temperature Gradient Differential Thermal Mass Flow Sensor"; also US Patent # 6,595,049B1 "Thermal Mass Flow Sensor with Improved Sensitivity and Response Time."

Thomas O. Maginnis, Ph.D. Physics of High Performance Sensors, P.O. Box 4029, Anaheim, CA 92803, 714-225-7996, sensorscholar@gmail.com.

This paper was previously presented at the Measurement Science Conference (MSC) in Pasadena, California, March 14-18, 2011, www.msc-conf.com.

Leveraging LEAN in the Laboratory

Dean S. Williams
Duke Energy Standards Lab

What do you do when faced with a doubling of demand with virtually no increase in resources? Go LEAN. That was the approach Duke Energy's Standards Lab took when it faced that situation recently. As a result of a merger with Progress Energy, which formed the largest investor owned electric utility in the U.S., the Duke Energy Standards Lab's customer base immediately doubled; but the staffing only increased by 10%. The merger and other cost cutting measures were a direct result of the changing landscape for electric utilities. As a result of the recent recession, the demand for electricity dropped and is only projected to grow minimally over the next 4 to 5 years. This fact, coupled with increasing costs due to aging infrastructure and new regulatory requirements has made belt tightening a necessity. The Duke Energy Standards Lab needed to change or fall prey to the alternative. As W. Edwards Deming so aptly described the situation, "It is not necessary to change. Survival is not mandatory."

The challenge the Standards Lab faced, which is all too common, is how, in the absence of corporate initiatives and within an already stretched budget, do you find the resources or time to implement a successful process improvement effort? The truth the Standards Lab team discovered was that by simply applying a few of the many process improvement tools available in the LEAN toolbox they could get well down that road. And this was the approach the Standards Lab initially took. Utilizing information gleaned from articles on the Internet and a careful reading of Lean for Dummies they embarked on their journey towards process improvement. They started applying a few of the tools and found them to be profoundly effective. Later in the process they were fortunate enough to get help and encouragement from Invistics, an Atlanta based LEAN consultancy, and the recently formed LEAN Process Improvement group within the newly merged Duke Energy. These resources showed the Standards Lab how to more rigorously apply the tools and techniques to get even better results.

What is LEAN?

In 1998 James Womack and a team from MIT were investigating the practices of the international automotive industry and found that Toyota Motor Company had processes that were producing unique results (these process became known as the Toyota Production System or TPS). Toyota's approach was essentially to focus on producing a quality product for their customers with a deliberate emphasis on reducing the amount of time, materials, inventory, and injuries it took to do the job. The codification of this approach was dubbed "LEAN"; the ability to accomplish more with less.

But the Standards Lab soon learned LEAN was not just about doing more with less, it is a philosophy that is rooted in the belief that customers determine what represents "value," and that whatever does not contribute to that value is "waste." It is also a philosophy that values the employee and does not want to waste their skills, knowledge, or talents.

The first step for the Standards Lab was to learn about wastes that might be clogging up their workflow stream. Based on the premise that waste is anything that does not provide value from the customer's perspective they discovered waste generally fell within 2 broad categories and came in many different forms. The first category was called Type 1 waste; activities that are non-value added (from the customer's perspective) but are somehow necessary. Take for example, employees filling out timesheets, or the company paying its taxes. Both of these may be required to keep the company running or keep you out of jail, but from a customer's perspective they do not add value to the product or service provided. Type 2 wastes are those activities that are non-value added and are not absolutely necessary. The trick the Standards Lab learned was to identify and categorize the wastes and deal with each accordingly. The goal was to completely eliminate all Type 2 waste and to reduce the effort and time it took to accomplish Type 1 waste.

The Standards Lab learned that, especially for Type 2 waste, it can take on a number of forms; referred to collectively as the "8 Wastes of LEAN." They used an easy to remember mnemonic, "DOWNTIME" to help them remember the 8 Wastes. As they reviewed the forms of waste they found the following:

Defects – Errors made during set up for a calibration or incorrect information on a certificate or label during the calibration process. Anything that could cause rework fits this form of waste.

Over Production – Calibrating instruments that are not being used in the field. These were often items that have been replaced by newer instruments, but have never been removed from the system.

Waiting – Instrument waiting for the next step in the process; technicians waiting on instructions, repair parts, or a standard. This type of waste led to longer turn times. In fact it was contributing to up to 80% or 90% of the average turn time.

Non-Utilized Talent – Failure to gain employee's unique perspective on the operation and insights into how to streamline the process. When not actively engaged that talent was untapped.

Transportation – Moving instruments and paperwork unnecessarily from one location to another as it moved through the process; trips the technician made daily to retrieve and return an instrument, or drop off a completed test report. Round trips could result in valuable minutes away from the calibration bench.

Inventory – Excess instruments and records in the system from unused standards to redundant paper files.

Motion – Steps undertaken in completing a task that didn't directly add value; trips to a remote printer to pick up the calibration certificate; data that was handwritten and then re-entered electronically.

Extra Processing – Taking more data points than necessary for a particular instrument type, or having too short a calibration interval based on the instrument's past performance.

The Standards Lab had to look for these wastes in all their processes; asking themselves whether each step or activity would be adding value from the customer perspective. They discovered the harsh reality that other than the actual bench calibration most everything else was either Type 1 or Type 2 waste.

8 WASTES

Defects
Over Production
Waiting
Non-Utilized Talent
Transportation
Inventory
Motion
Extra Processing

Starting the Improvement Process

With knowledge of the wastes in hand and an understanding of value from the customer's perspective the Standards Lab was ready for the next steps in applying LEAN tools to make improvements. They needed to go to where the work was being performed and just observe the workflow and activities. In Japanese this "going" and "observing" is referred to as "Gemba" and "Genchi Genbutsu." Expressed differently by that great American philosopher Yogi Berra, "You can often see a lot just by looking." The Standards Lab team found that a helpful tool to utilize at this point was the Spaghetti Diagram. Spaghetti Diagrams are a simple visual representation of how a person, product, or paperwork physically moves through and about the facility. By plotting every movement from start to completion a jumble of lines often emerged that looked like a pile of spaghetti. They found this was a great way to capture motion waste that individuals might not consciously be aware was occurring.

Another technique the Standards Lab employed in the initial data gathering phase was the 5 Whys technique. This is a simple root cause analysis that involves asking "Why?" as many times as necessary to get to the underlying issue or the basis (or lack of basis) for any activity that is part of the current process. Usually no more than 5 "whys" were necessary to get to the bottom of an issue or find why something is really being done. What they found was that some activities were a left over step from a prior process that no longer served a value added purpose. These activities were like the woman that always cut the end off the hambone before putting it in the oven. When asked by her 5 year-old son "why" she did it, she said, "I'm not sure, but this is how grandma always did it." As grandma was there for Easter dinner the boy went and asked her "why?" Her answer was simple, "When your mom was growing up we had a very small oven in our apartment and it was the only way I could fit the ham in the oven. I have no idea why, with that big oven your mom has, that she is still cutting the end off the hambone." The 5 Whys technique helped the Standards Lab identify those hambones.

Focusing In On Making Improvements

With some basic data and a good first hand look at how things were actually being done it was time for the Standards Lab to look for ways to improve the process. The first step was to develop some Value Stream Maps. Value Stream Maps are a simple graphic layout of workflow activities. The Standards Lab team used long paper sheets taped to a wall with sticky notes used to record the individual steps, activities, and decision points.

These maps were developed on several levels, each serving a slightly different purpose. They first developed one that looked at the overall major calibration process steps: receive the instrument, perform the calibration, document the results, approve the report, and ship the instrument. By document the average time it actually took to perform each step, adding those together, and subtracting it from their average turn time they were shocked to find that instruments spent about 90% of their time at the Lab waiting between steps. By coming up with strategies to reduce those wait times they were able to cut their turn times in half.

Another map was developed with the help of the consultants from Invistics. This map looked at the different value streams within the process. This helped the Standards Lab identify categories of instruments that would benefit from different scheduling strategies. Instruments for which there were limited quantities were automatically moved to the head of the line, ensuring the quickest return to service date. Other items for which there were larger quantities could be batched and calibrated at the same time to optimize set up efficiency.

The third set of maps were detailed process maps developed for each of the areas within the overall operation, including the various Lab areas and the shipping/receiving area. The corporate LEAN Process Improvement group was instrumental in facilitating this effort allowing the Standards Lab to complete 10 area maps in just a few days. This effort involved everyone within the Standards Lab's organization, ensuring employee's insights into the details of the process were captured.

For each area a "current state" map was developed which documented each step or activity that was currently involved in completing tasks. It was important to get everyone's involvement, because, like the various witnesses at the scene of an accident, each one remembers different aspects. Many times during the process someone would note, "Oh, before we do that don't we always…" These afterthoughts often reflected small, but incremental wastes contained within the process.

The next step was to create a desired "future state" map. To do this the Standards Lab employees familiar with the process were each given red, yellow, and green sticky dots. Based on their understanding of the types and forms of waste they were asked to place the dots on the current state activity steps accordingly:

- red dots were placed on each step that they thought was "Un-Necessary and Non-Value Added";
- yellow dots on each step that was "Necessary, but Non-Value Added"; and,
- green dots on the truly "Value Added" steps.

For steps where different individuals placed different colored dots, the item was discussed until consensus was reached. By removing the red dot items and giving careful consideration to how to most efficiently perform the yellow dot items a new future state map came into focus. When completed, it was reviewed one more time to validate all the assumptions and make sure no steps were left out, and as importantly, no waste left in.

Torque/Force Before 5S

There was one final step in the process. For all the changes that were being recommended a list of priorities was established. The items that would give the most bang for the buck were balanced against how achievable it would be to implement the items given the time and resources currently available. While the goal was to implement every idea, the Standards Lab learned that implementing LEAN is sometimes like eating an elephant, you need do it one bite at a time.

5S Kaizen Events

With a basic game plan in place, the next step for the Standards Lab team was to start putting some feet on the project. This involved conducting 5S Kaizen Events in each area using the data that was previously gathered, spaghetti diagrams, and the future state maps. As the name implies, this involved taking a fresh look at each work area and systematically preparing it for increased effectiveness using a 5-step process. Those steps were:

- **Sort** – In each work area they removed everything that was not literally bolted to the floor, pulled it out of the Lab, and sorted it based on the 3 "Rs." Retain it if it is absolutely necessary to perform the work in that area, Return it if it is something that properly belongs in another area, and Rid yourself of it (trash or recycle) if it doesn't directly serve a current value added purpose.

Torque/Force After 5S

- **Shine** – The Standards Lab undertook a thorough "spring cleaning" of each area. This made for a more inviting and safer work environment and sent a message that with LEAN things were going to be first class. As an added step, each Lab area had one wall repainted with an accent color to match the new company logo colors. This further reinforced the message that the Standards Lab was to play an important part in the future success of the company.
- **Straighten** – As items were returned to freshly cleaned and painted areas careful consideration was given to the optimal location. They considered motion and transportation waste and looked for ways they could be eliminated or minimized. Process constraints were removed. One notable example was in the Pressure Lab where each new pressure controller that had been purchased over the years was neatly place one on top of the other in a metal cabinet. The technicians had pointed out that while it looked nice with this configuration, only one of the units could be used at time. The controllers were put back side-by-side on a counter top and spaced out in a manner that eliminated the constraint.
- **Standardize** – Instead of a mish-mash of hand tools scattered among various drawers and cabinets, a complete set of only those tools necessary to support the work in that Lab were returned. These were organized and conveniently located at each workstation, and the drawers labeled to ensure items could be easily found and, as importantly, had a specific home to returned to when not in use.
- **Sustain** – The corporate LEAN Improvement Team leader reinforced that this step in the process was necessary to ensure the newly renovated and redesigned Labs would remain in tip-top shape. The team developed an audit checklist and scorecard to use when auditing the condition of each area. Initially audits were performed more frequently until new habits were adopted. As these new habits were established audits were performed less frequently, with the team finally settling on an optimum monthly interval. Each Lab got a score and a "radar chart" was posted which graphically showed their performance on 5 spokes corresponding to the 5S's of the event. Trend charts of each Lab's monthly scores were posted in the break area so performance to standards was clear for all to see.

The results were dramatic. Hundreds of unnecessary items were removed from the Labs, space was freed up and standards, tools, consumables, and workstations were optimized to match the future state maps developed earlier.

Continuous Improvement

With all these improvements under their belt, the Standards Lab team was proud of their achievements. But it soon became apparent that process improvement was not a destination, but a continuing journey. So the Standards Lab Team has started to go back through each area and further refine processes. A new culture has emerged where team members are regularly coming forward with improvement ideas, "What if we moved the printers over here. That could save several steps during each calibration," or "Do we really need to perform this step, is it really adding value," or "This seems like a necessary, but non-value added step, couldn't we streamline the process by…"

All of the above, and the implementation of "Pull" workflow, another LEAN tool, has allowed the Standards Lab to meet the new challenges head on; taking on more calibrations and doing so without increasing the cost. Using some simple LEAN tools the Standards Lab has now increased its throughput per technician by over 400%, without any increase in overtime. If future mergers come to pass, the Standards Lab team is confident they can meet those challenges in the same way.

Dean S. Williams, Manager, Duke Energy Standards Lab, Huntersville, NC, Dean.Williams@Duke-Energy.com.

Thoughts on Metrology Software Life Cycles

Michael L. Schwartz
Cal Lab Solutions, Inc.

I was having a long conversation the other day with a fellow software engineer. One of the topics we talked about for hours was software life cycles and how metrology software is not like most software. One big difference is the typical life cycle of metrology software; most software applications have a short life cycle, usually less than five years. But when it comes to metrology software, many of the application we are running today are more than twenty years old. That is four times the natural life expectancy of software.

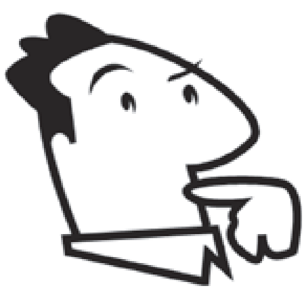

For those of us who have been in this industry for years there are a few names that stand out. One good example is Hewlett Packard's Rocky Mountain Basic (RMB). Born in the late 1970's it was introduced as a tool for scientists and engineers to control instrumentation. It was then later embedded in the instrumentation hardware. I remember how cool it was to write custom software that would run right on the measurement hardware. And still today, when I visit calibration labs I see Rocky Mountain Basic procedures running and being developed.

So why is it that very few software applications running on my computer are more than five years old, while the software we are running in the lab is ancient? Why do companies rewrite, rethink and drastically update software? And why does this not happen as often with metrology software?

All of this got me to thinking, "What is the life cycle of metrology software?" If I was to write something new today, how long would it be used? But most importantly, what could I do today in designing my software that could impact its longevity? All difficult questions, but none the less they should be part of our design paradigm.

What is the life expectancy of metrology software? I think to answer this question we have to take a good hard look at the life expectancy of the hardware we are running. Taking a step back and looking at the total picture, it becomes obvious that it's not the software but rather the measurement hardware's longevity extending the life expectancy of software. I am amazed to still see calibration labs using standards that are 20 years old. Often when I ask a calibration lab why they are using such old standards the answer is usually related to historical data or accuracy.

New standards are being created every day, but I have noticed a trend; the greater the accuracy of a standard, the longer its life expectancy. There are many examples, just look around your calibration lab. Most labs will have a 57xxA, 3458A, 8510C, 8902A—all standards engineered and designed more than 20 years ago. In many labs today, they are still the calibration lab's primary traceable standards.

There is a direct relationship between the long life cycle of metrology software and the accuracy of the lab standards. Most software is directly tied to the computers they run on; when we replace the computer, we install all new software. But in the metrology world, we will install old software on a new computer because it makes good measurements.

So when designing our software, we must to plan for the super computers of the future. As Moore's Law continues to hold true, we know the computing power controlling our measurement hardware will be magnitudes more powerful in just a few years. We have to factor in speed consideration for tomorrow's computers when designing the software. Then we need to find that balance between measurement accuracy and speed.

Speed itself is a double edged sword. Faster computers can cause the software to run to fast, causing errors in measurements. We need to resolve those speed issues before they result in measurement errors. Adding a wait statement is one solution, but then how much processor is going to be wasted waiting for time to pass?

Metrology as a science is well established with a bright, long lasting future. When choosing a language we should look for the same things, such as languages that are widely used and accepted in all industries. Cross platform support will also maximize longevity. Languages like C#, Java and LabView have all been widely used and accepted and, at present, show no signs of losing ground.

Organizing and architecting software for both today's use and tomorrow's unknowns is extremely difficult. I have found avoiding specifics and thinking in abstract layers leads to better software design. The more specifics you can push down to the lowest possible level, the more robust your code will be. And the more robust your software is, the greater the chances are it will still be running long after you are gone. ❧

ISOTECH

The World Leader in Temperature Metrology

Thank you for making ~~2012~~ 2013 our best year yet.

More Nations Choose Isotech Temperature Standards.... Shouldn't You?

Thermometry Bridges 0.017mk to 0.5mk

Calibration Baths & Furnaces -196°C to 1300°C

Portable Temperature Sources -100°C to 1300°C

Thermocouple Referencing Systems

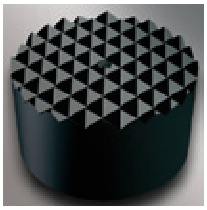

Blackbody Sources High Emissivity to 1300°C

Primary Temperature Standards

Reference Thermometers 0.001°C to 0.02°C

Isotech North America *(The Americas)*
Web-site: **www.isotechna.com**
E-mail: sales@isotechna.com
Phone: +(802) 863-8050

Isothermal Technology Limited *(Worldwide)*
Web-site: **www.isotech.co.uk**
E-mail: info@isotech.co.uk
Phone: +44 (0) 1704 543830

DISCOVER THE "BLUE BOX" DIFFERENCE™

6650A DUAL SOURCE HIGH RESISTANCE METER

- Replaces Teraohmmeter/ Electrometer Technology
- Range 100kΩ to 10PΩ
- Direct Reading or Live Ratio mode
- Any Ratio up to 100:1 Ratio
- 1V to 1000V Variable Output
- Automatic Scanner Control
- Surface and Volume Resistivity
- Voltage and Current Measurements
- Low Cost of Ownership

Measurements International
Metrology is Our Science, Accuracy is Our Business™

www.mintl.com